Ivan Fumagalli

Special Course "*Mathematical modeling of the human brain: from physiology to neurodegenerative disorders*"

Università degli Studi di Roma Tor Vergata

22 January 2025

The BraiNum project

brainum.mox.polimi.it

lymph

lymph.bitbucket.io

Clinical collaborations with:

Fondazione I.R.C.C.S. Istituto Neurologico Carlo Besta

IRCCS HUMANITAS RESEARCH HOSPITAL

Paola F. Antonietti (P.I.)

Mattia Corti

Ivan Fumagalli

Caterina Leimer Saglio

Niteen Kumar

Stefano Pagani

Francesca Bonizzoni

Nicola Parolini

Recap – numerical modelling of the brain function

Poromechanics and CSF flow, waste clearance

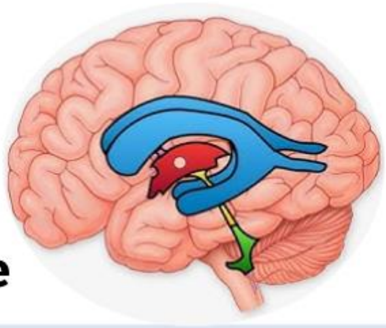

Distribution of misfolded proteins

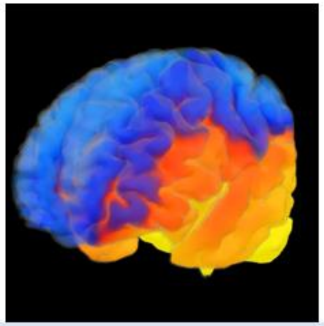

Neural axon degeneration and brain remodeling

TIME

$\sim 10^{0}$-10^{4} **s (heartbeat-hours)**

$\sim 10^{7}$ **s (years)**

$\sim 10^{8}$ **s (decades)**

SPACE

proteins $\sim 10^{-9}$ **m**

neuronal axons $\sim 10^{-6}$ **m**

organ scale $\sim 10^{-1}$ **m**

Recap – numerical modelling of the brain function

CSF flow

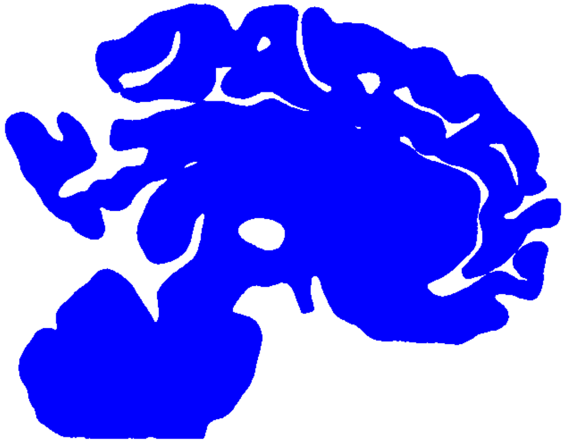

Signal propagation

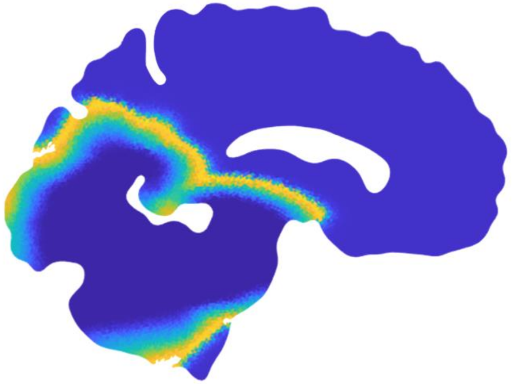

courtesy: C.B.Leimer Saglio

Protein spreading

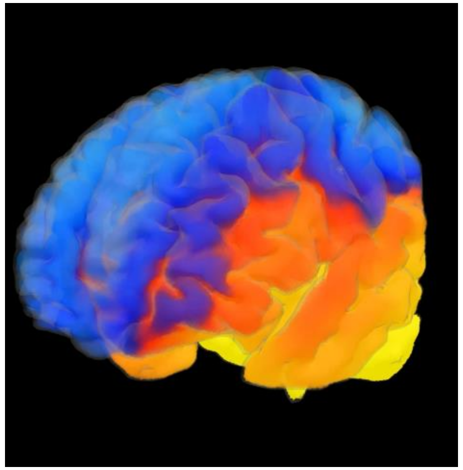

courtesy: M. Corti

Hemodynamics

courtesy: E. Irali

...all need a computational domain (mesh)

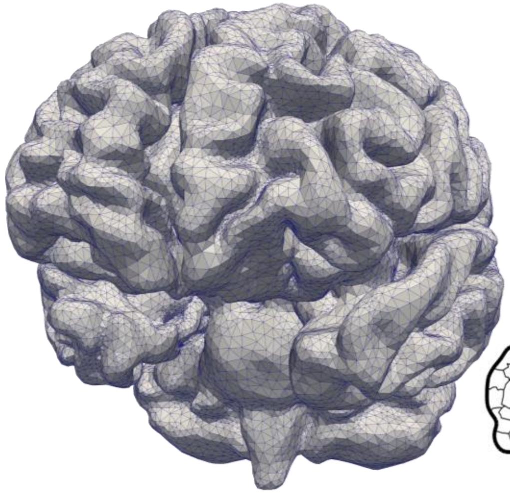

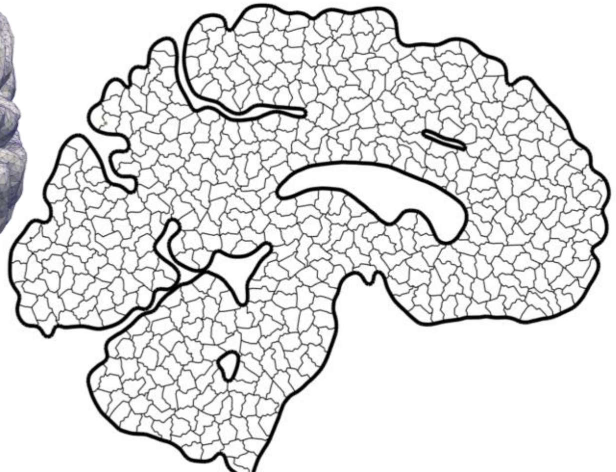

Geometric domain and data

Computational studies can be performed in

Idealized and/or average models

- ✓ Parametric studies
- ✓ Benchmarking and verification
- ✓ No image segmentation required
- • Real geometry not available
- x **Geometrical features** may have major impact on results
- x Following **time evolution** of pathology not easy

Patient-specific models

- ✓ **Actual** patient’s condition (e.g. atrophia)
- ✓ Can follow **pathology development**
- ✓ Include non-pathological **anomalies**
- • Real geometry available as imaging data
- x Need of accurate/appropriate data
- x Reconstruction/calibration may be **time expensive**

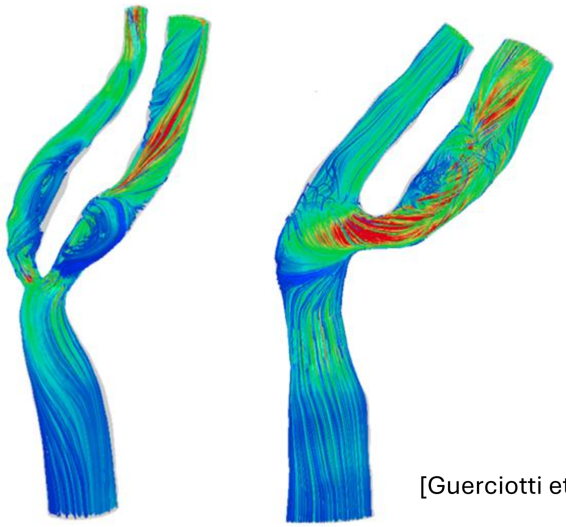

[Guerciotti et al. 2017]

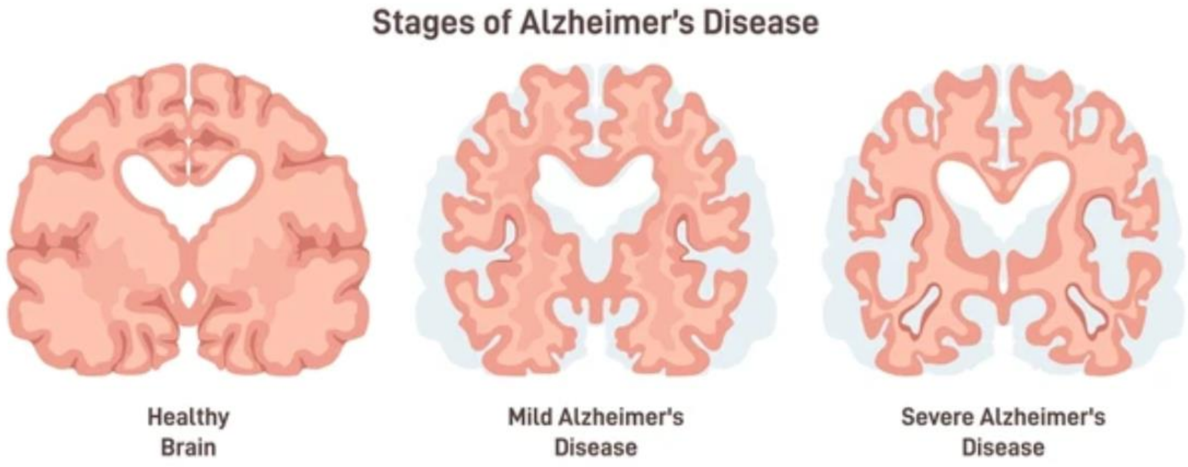

Workflow: from images to computational mesh

Imaging data

MRI

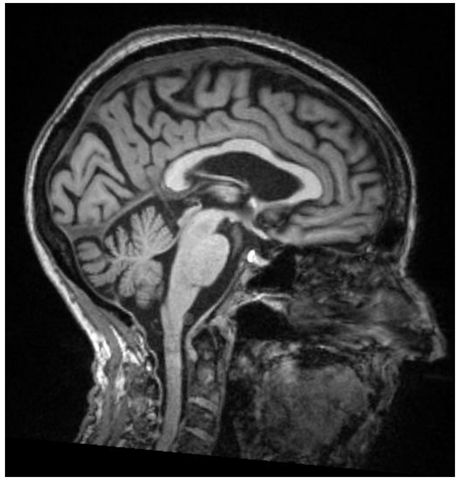

angiography

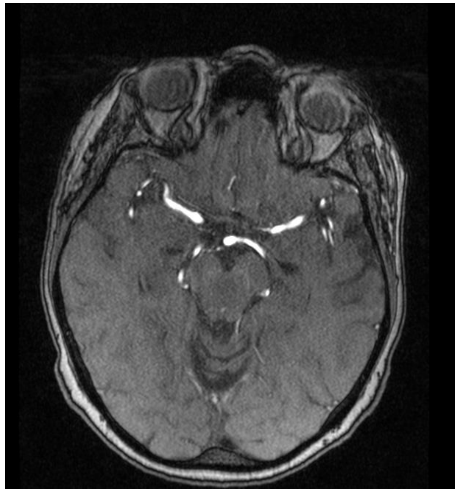

Domain reconstruction

Mesh generation

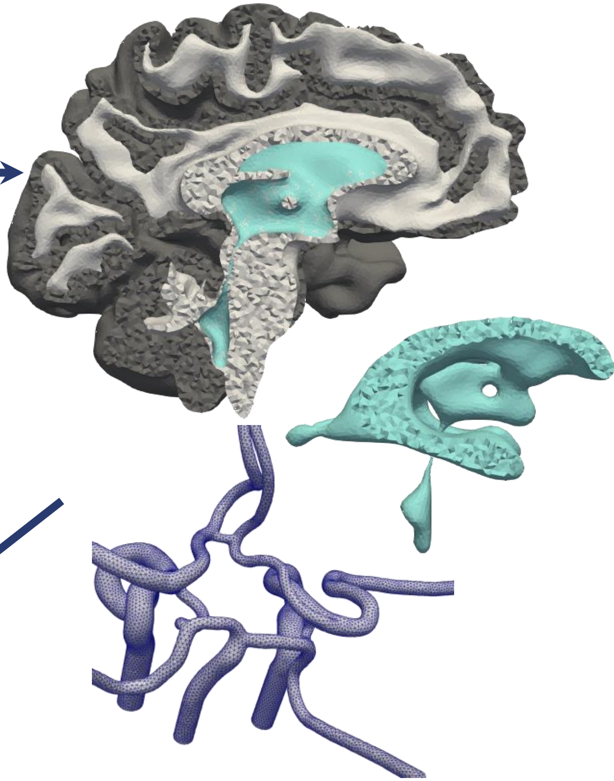

Agglomerated poly grid

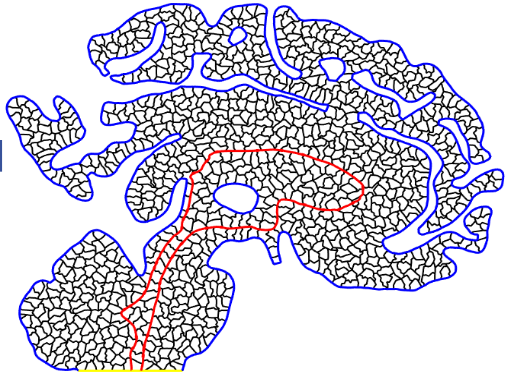

OASIS-3 database https://oasis-brains.org/ [LaMontagne, Benzinger, Morris et al. 2019]

Contents

Material

Shared OneDrive folder:

https://tinyurl.com/LabBrain2025

You can find data and results of the reconstruction part of this lecture.

Docker image with all the requirements for brain mesh generation:
https://hub.docker.com/repository/docker/ivanfumagalli/my-svmtk

About the data

The T1-weighted MRI data uploaded in https://tinyurl.com/LabBrain2025 is taken from the OpenNeuro database [http://openneuro.org], in particular from subject 087 of project *ds004471* [M. Abbass, G. Gilmore, A. Taha, R. Chevalier, M. Jach, T. M. Peters, A. R. Khan, J. C. Lau (2023). London Heath Sciences Center Parkinson's Disease Dataset (LHSCPD). OpenNeuro. [Dataset] doi: 10.18112/openneuro.ds004471.v1.0.1

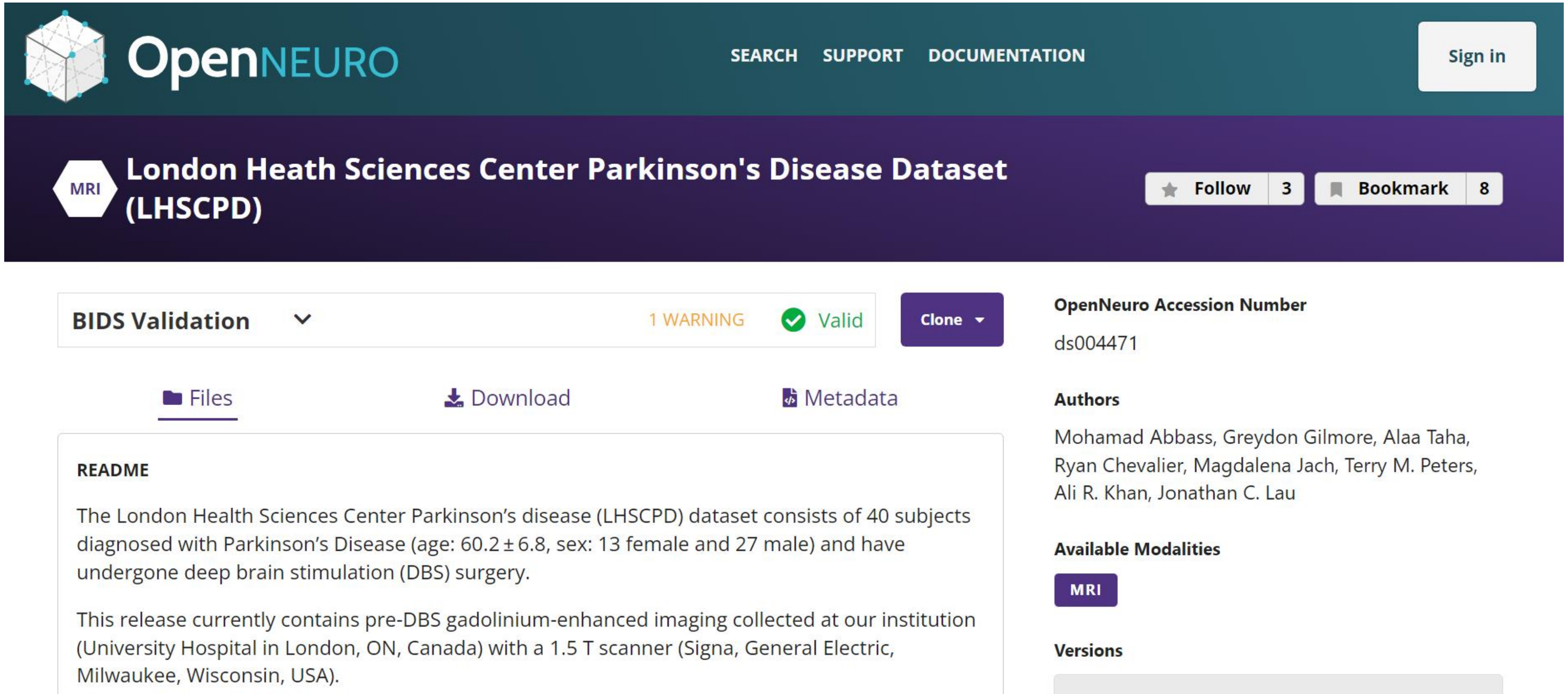

1 – Imaging data in a nutshell

Computer Tomography (CT)

Diagnostic imaging procedure that combines multiple cross-sectional (*tomographic*) X-ray acquisitions and digital geometry processing to generate a **3D volume** of the inside of the body, made of **pixels**.

Grey values represent the attenuation coefficient (strictly related to **density**) of the tissues, expressed in Hounsfield units (HU)

- Air: -1000
- Fat: -100
- Water: 0
- **CSF: 15**
- **White matter: 20-30**
- **Blood: 30-45**
- **Grey matter: 37-45**
- Muscle: 40
- Bone: 700-3000

Wikimedia Commons – lic. CC0-1.0 Mikael Häggström, M.D.

✓ Great **space resolution**: ~1 mm (even ~100 μm for high-res. machines)

✓ Relatively quick acquisition (few minutes)

x Radiations can be damaging

x Very limited time series

Magnetic Resonance Imaging (MRI)


Wikimedia Commons

Diagnostic imaging procedure based on the application of heterogeneous and time-varying magnetic field: based on magnetic relaxation properties of the hydrogen nuclei contained in the tissue, construct a **“3D” volume** (actually an array of **“2D” slabs**) of the inside of the body, made of **voxels**.

Grey values represent the **magnetic relaxation time** of the tissues:

T1-weighted MRI
relaxation time of
longitudinal ma

MRI is the gold standard in clinical practice, routinely employed in diagnosis and follow-up

T2-weighted M
relaxation time
transverse mag

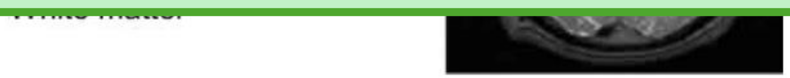

[R. A. Pooley, Radiographics 25 (2005)]

- ✓ **Non-invasive** (no radiations – except if contrast agent is used)
- ✓ **Highly parametrizable**:
  - allows different orientations
  - different acquisition protocols yield **different contrast**
- Longer scan time w.r.t. CT
- Resolution: **1-3 mm**

Functional Magnetic Resonance Imaging (fMRI)

Employs the techniques of MRI to measure **oxygen levels** in the tissue.
Function is measured relying on the Blood Oxygenation Level Dependent (**BOLD**) phenomenon:

neuronal activation ⇨ increased blood flow ⇨ increased oxygenation

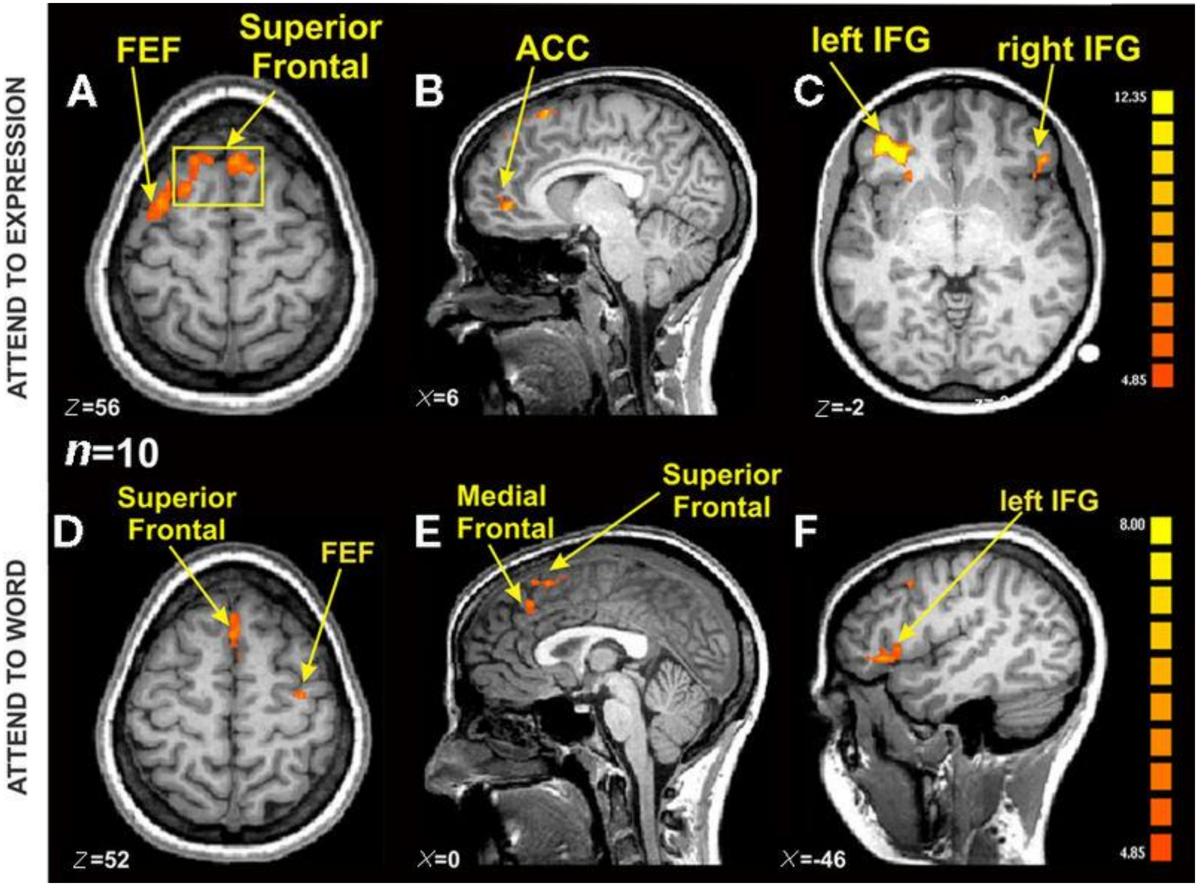

- Measures **function**, not anatomy
- Clinical applications:
  - mapping motor and language areas, and their impairment
  - fMRI-guided neurosurgery

Angiography

General naming of a technique used to visualize the inside (***lumen***) of **blood vessels** and cavities.

- Traditional angiography: X-ray based techniques in combination with radio-opaque contrast agent
- Now, typically obtained from CT or MRI

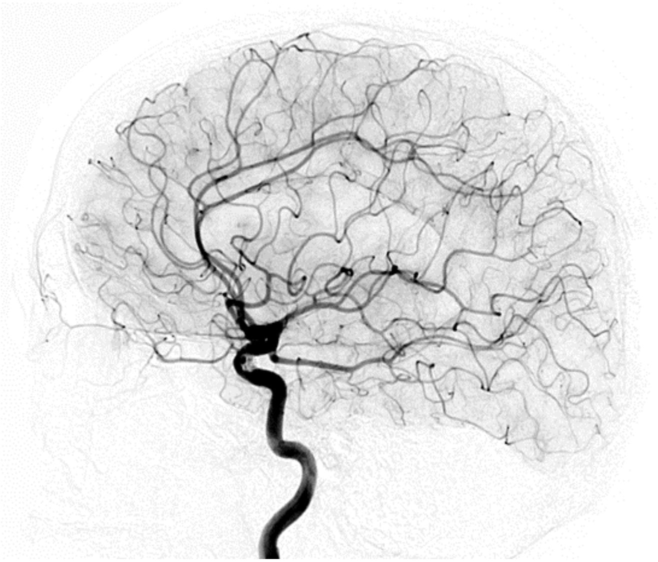

Traditional cerebral angiogram

CT coronary angiogram

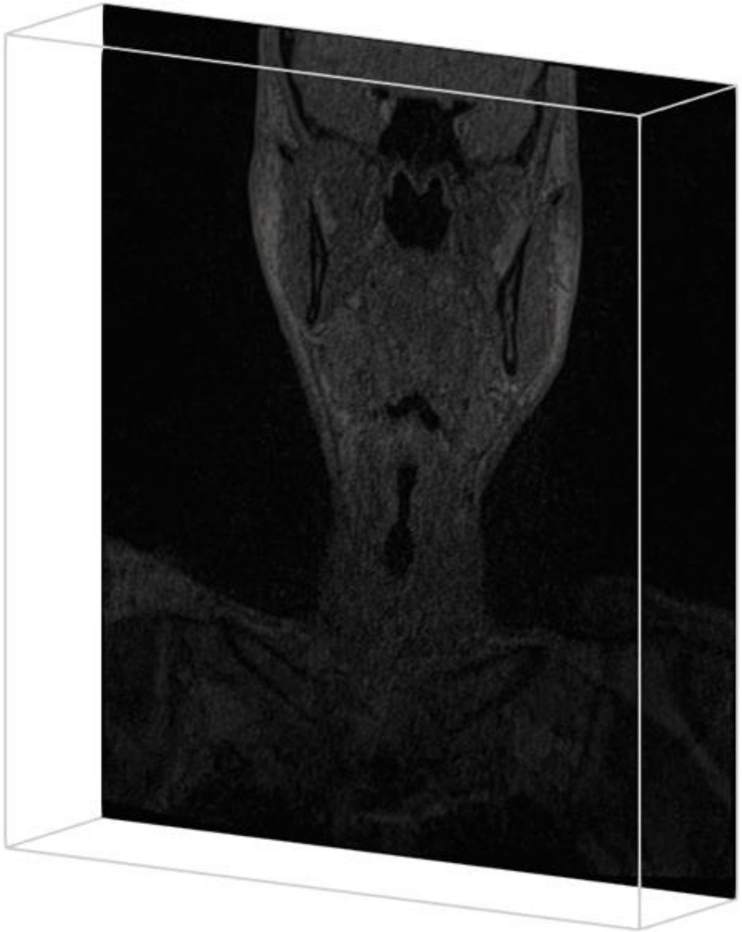

MR angiogram of neck and basal cranial vessels

Other acquisitions for specific tasks

Diffusion-tensor MRI (dt-MRI)

Used to measuring the diffusion of water molecules through livin tissues

⇨ highlight areas of activity

⇨ allow reconstruction of **neuronal fibers**

⇨ used also for myocardial fibers (ex vivo)

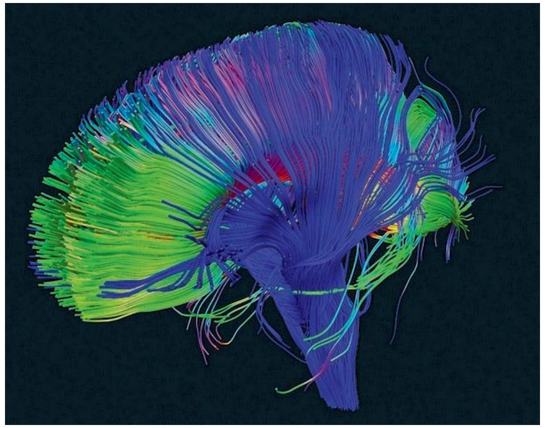

Credit: NICHD/P. Basser

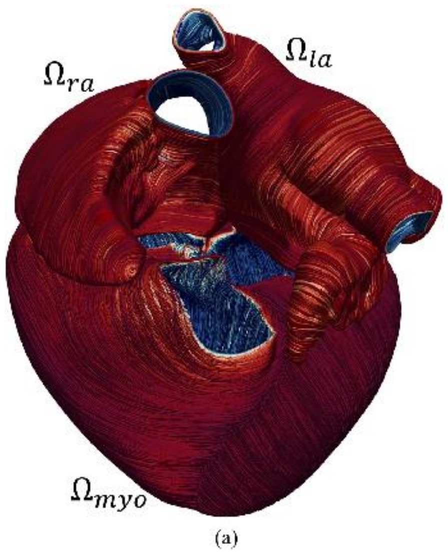

[Piersanti et al. CMAME 373 (2011)]

Positron Emission Tomography (PET)

A positron-emitting agent is injected in bloodstream. Radioactivity is affected by biochemical processes: it can identify functional anomalies:

⇨ used to detect tumors and amyloid deposits

⇨ limited use due to radiations

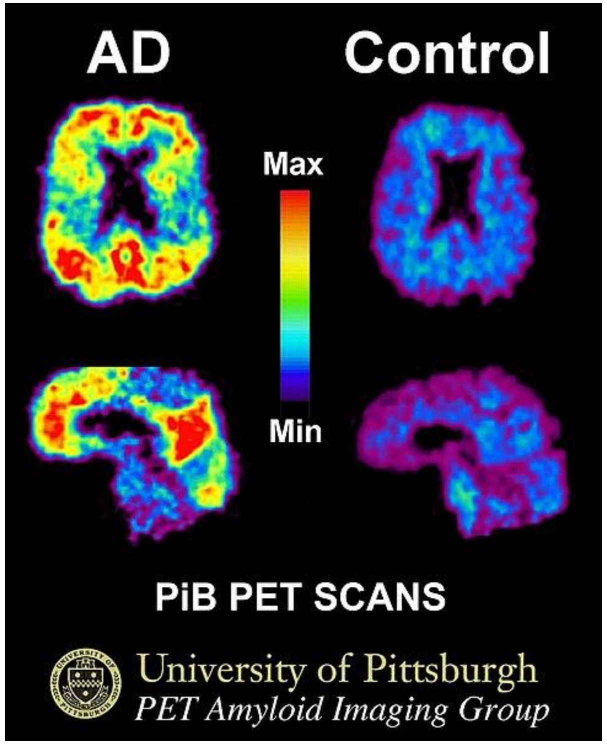

Wikimedia Commons - lic. CC-BY:SA 3.0 Klunkwe (2008)

Possible issues - MRI

Partial Volume Effect (PVE)

More than one tissue type is comprised in a voxel

⇨ voxel intensity = (weighted) average

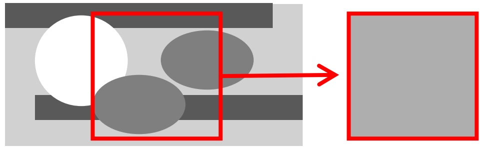

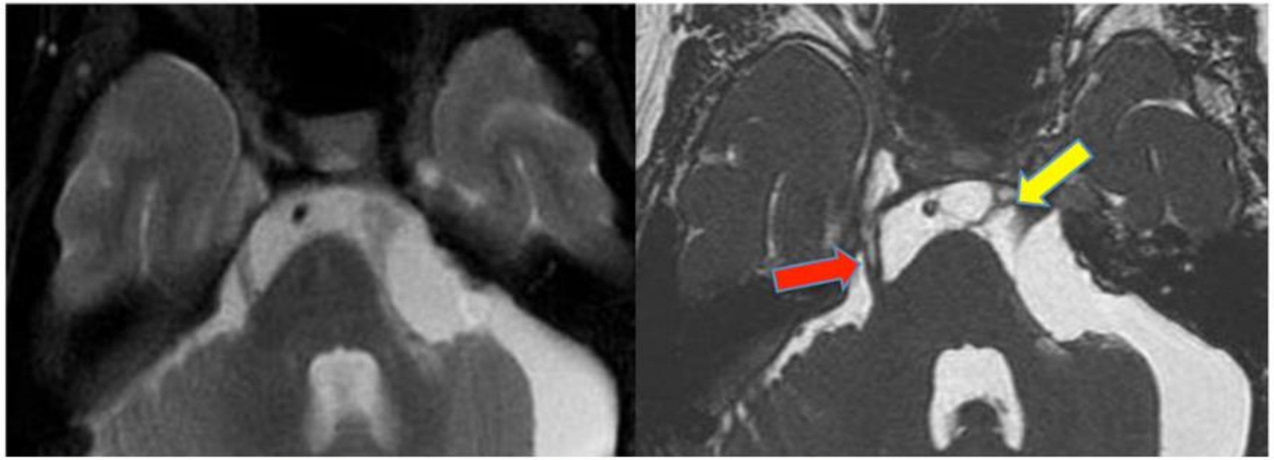

Partial volume averaging. In 5-mm-thick section (left) delicate nerves and scar in the subarachnoid space cannot be resolved as their signals are mixed/averaged with CSF and other tissues. Thin-section (1-mm-thick) image (right) displays the detailed anatomy to good advantage.

Cross-talk artifacts

Due to slab **overlap** (actual or due to no-gap)

⇨ contrast is impaired

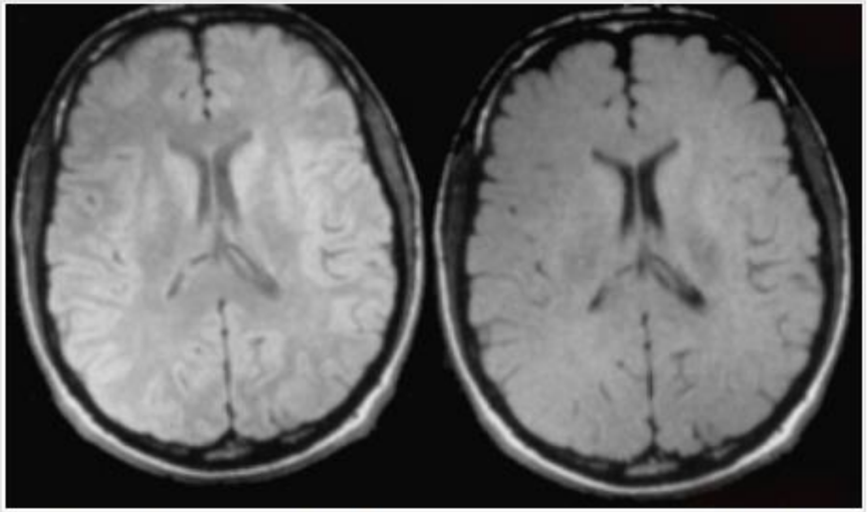

Effect of cross-talk on image contrast. On left is a SE 2000/20 image with 50% gap showing expected spin-density contrast. On right the same sequence with 0% gap demonstrating impaired contrast.

https://mriquestions.com/

Many image-processing tools are available (even integrated in scanning machines) to avoid/correct these and other issues. Yet, being aware of them allows to improve certified accuracy of the solutions.

2 –From images to computational mesh: a reconstruction pipeline

Overall workflow and tools

Imaging data

MRI

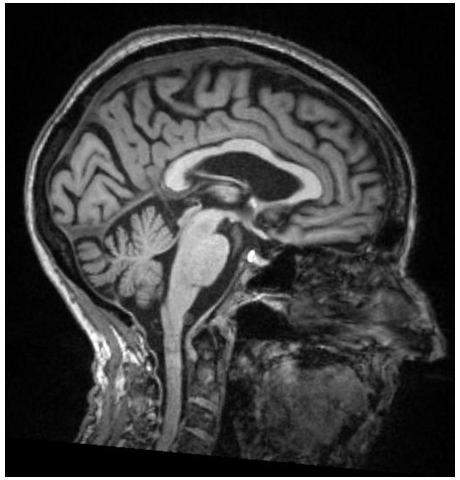

angiography

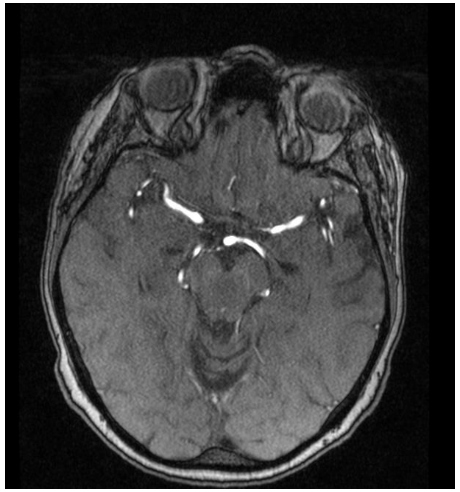

FreeSurfer

https://surfer.nmr.mgh.harvard.edu/

Domain reconstruction

SVMTK

github.com/SVMTK/SVMTK

[Mardal, Rognes, Thompson, Valnes (2022)]

vmtk

vmtk.org

github.com/checkrenzi/vmtk

Mesh generation

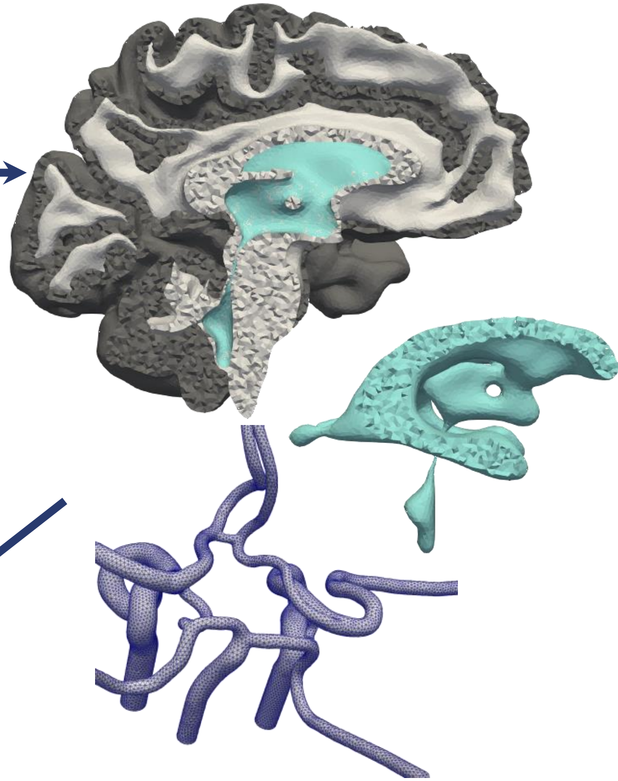

ParMETIS

Agglomerated poly grid

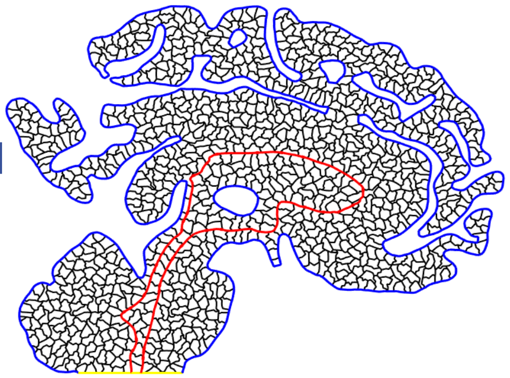

NB: Many other tools are available!

OASIS-3 database https://oasis-brains.org/ [LaMontagne, Benzinger, Morris et al. 2019]

2.1 – Segmentation of brain MRI

Segmentation techniques

- **Manual segmentation**
- Thresholding / isosurface
- Front propagation
  - Fast marching
  - Colliding fronts
- AI/ML/DL techniques
- Deformable models / registration
  - Level set method

Widely employed in clinical practice for **cardiac** imaging.

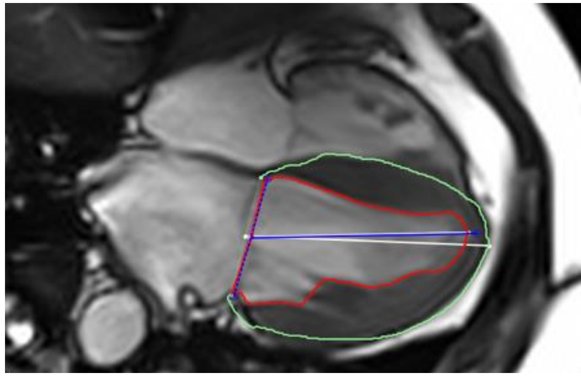

Little use for brain images: complex geometry and structures.

Only for:

- geometry sizing (e.g. tumors) of typically pre-processed images
- creating benchmark/**ground truth** templates for other techniques

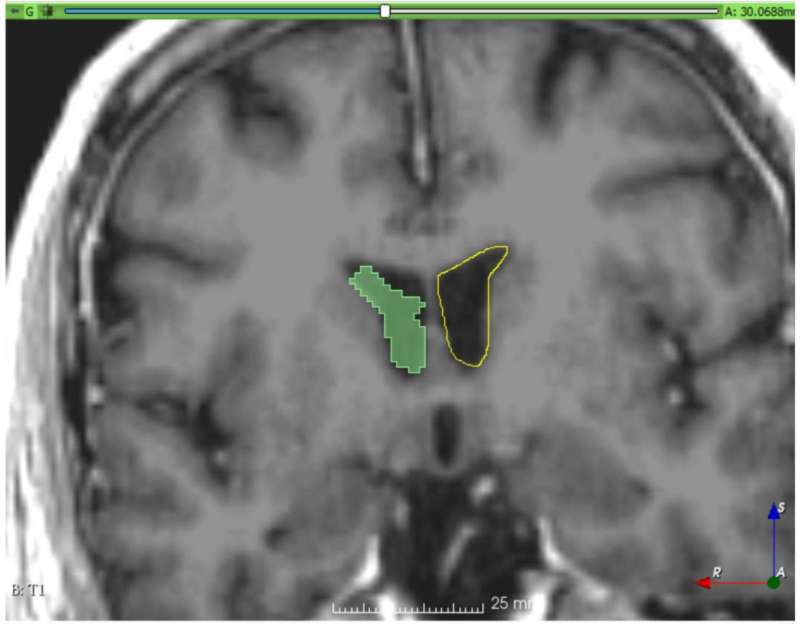

- Results (can be) accurate
- x **Time** consuming
- x Intra- and inter-patient **variability**
- x Requires **expert** knowledge of the district of interest

Segmentation techniques

- Manual segmentation
- **Thresholding / isosurface**
- Front propagation
  - Fast marching
  - Colliding fronts
- AI/ML/DL techniques
- Deformable models / registration
  - Level set method

Identification of a suitable gray **level** (isosurface) or **range** of values (region thresholding) to identify the region of interest:

- by relying on Hounsfield units (for CT) or other normalized ranges
- via suitable algorithms (e.g. Otsu's method based on intensity histograms)

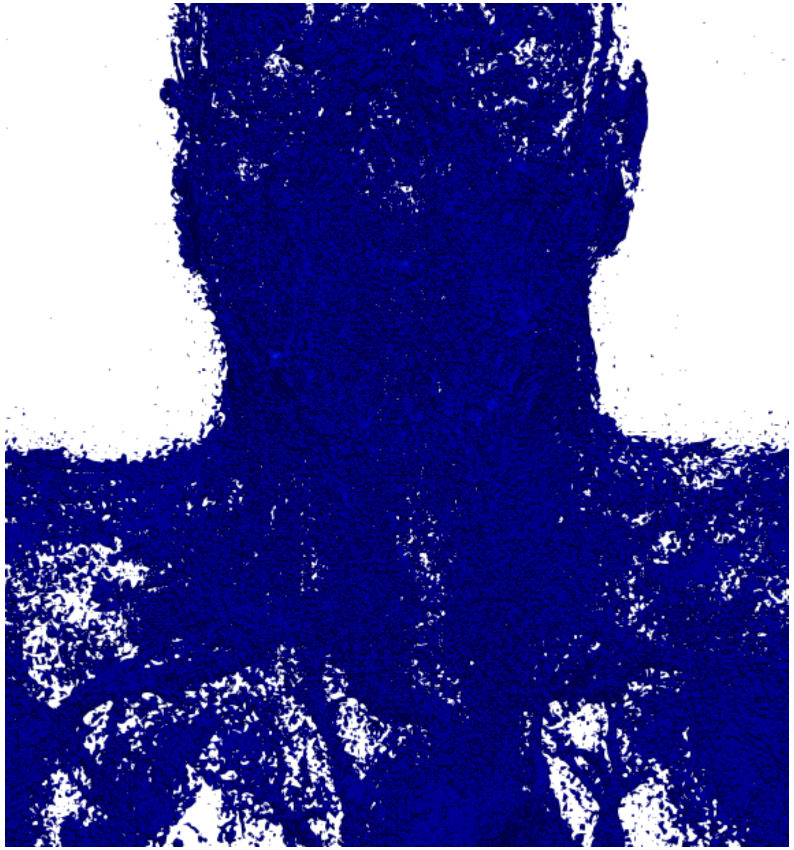

✓ **Fast**

✓ Good **initalization** for other techniques

x No control on shape

x Not robust w.r.t. patient's characteristics, anatomical features, scan protocol, contrast agent…

Segmentation techniques

- Manual segmentation
- Thresholding / isosurface
- **Front propagation**
  - **Fast marching**
  - **Colliding fronts**
- AI/ML/DL techniques
- Deformable models / registration
  - Level set method

Starting from an initial condition (e.g. obtained by thresholding), a wavefront is tracked (e.g. solution of a PDE or a graph-based advancing scheme).

Wavefront velocity typically **decreasing with the gradient of the gray level**:

(i.e. slows down close to the boundary of a uniform region)

- **Fast marching**: Front propagates from a source, stops when reaching a target

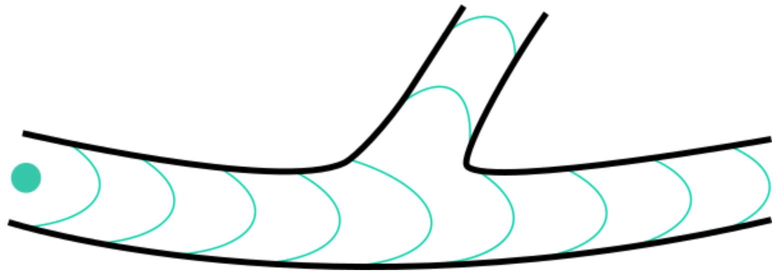

courtesy: L. Bennati

✓ Suitable for **round** objects / intricate **vessel network**

- **Colliding fronts:** Front propagates from multiple seeds

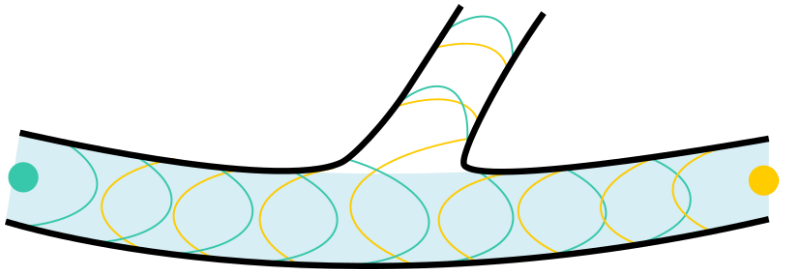

courtesy: L. Bennati

✓ Suitable for **single vessels**

x Not reliable for **complex bulk geometries** (e.g. grey/white matter)

Segmentation techniques

- Manual segmentation
- Thresholding / isosurface
- Front propagation
    - Fast marching
    - Colliding fronts
- **AI/ML/DL techniques**
- Deformable models / registration
    - Level set method

Based on the training of a neural network (or other filtering systems) mapping:

DICOM images → **segmentation masks**

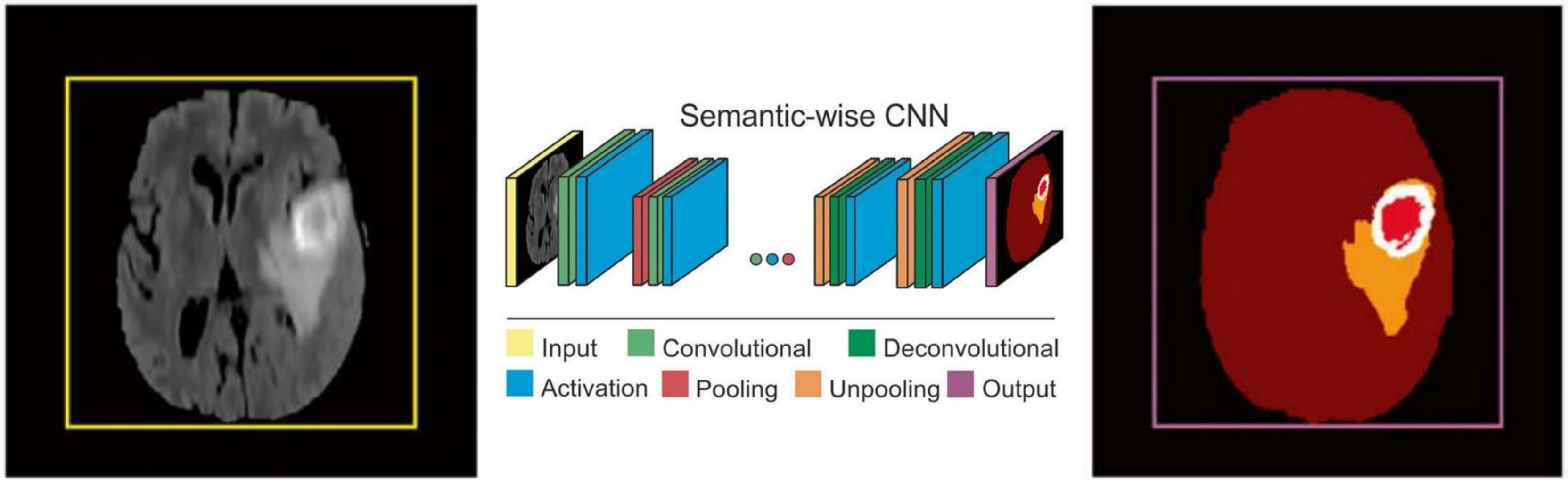

[Akkus et al. J Digit Imaging 30:449-459 (2017)]

Once trained, the model can automatically detect structures and segment.

✗ Training requires **large datasets** and significant time

✓ **Pre-trained and verified models available** on the market

Segmentation techniques

- Manual segmentation
- Thresholding / isosurface
- Front propagation
  - Fast marching
  - Colliding fronts
- AI/ML/DL techniques
- **Deformable models / registration**
  - **Level set method**

Surface is represented as the **zero-level set** of a function φ : $\Sigma = \{ \boldsymbol{x} \in \text{image} : \varphi(\boldsymbol{x}) = 0\}$

✓ Can use any other technique as initialization

✓ Tunable parameters for the trade-off between **smoothness** and **accuracy**

x Calibration can require multiple attempts, to avoid **over-smoothing**

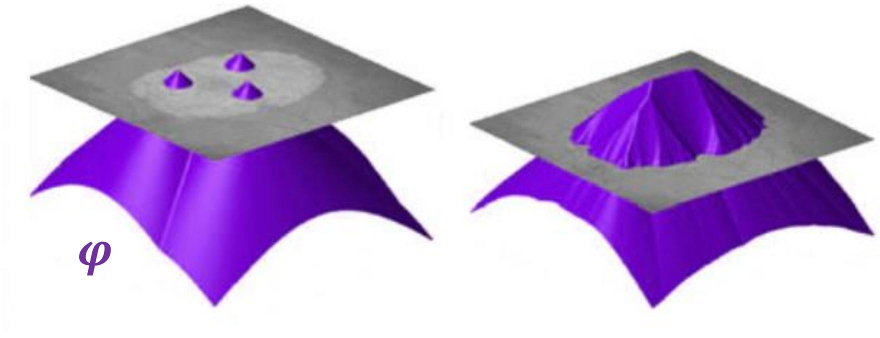

Given an initialization, the level-set function evolves as result of the balance between:

- internal forces: preserve the **smoothness** of the surface
- external forces: **gray level gradient** (slow down when approaching boundaries)

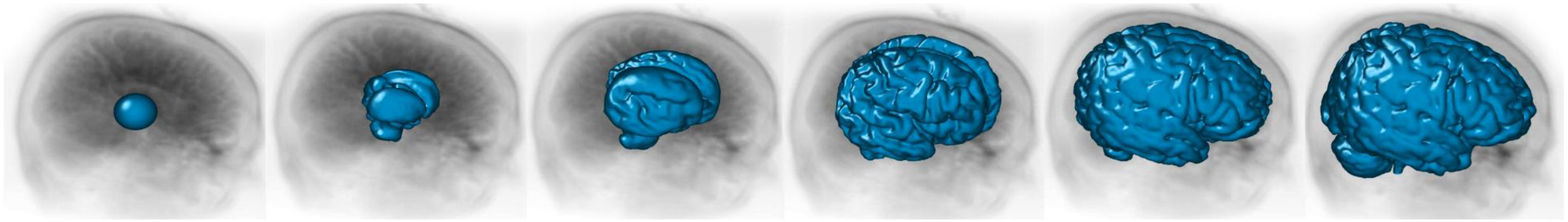

Automatic (pre-)segmentation of brain regions

*"FreeSurfer is a software package for the **analysis** and **visualization** of structural and functional neuroimaging data from cross-sectional or longitudinal studies. It is developed by the Laboratory for Computational Neuroimaging at the Athinoula A. Martinos Center for Biomedical Imaging. FreeSurfer is the **structural MRI analysis** software of choice for the Human Connectome Project."* [FreeSurfer wiki]

It is released under an open source license.

FreeSurfer

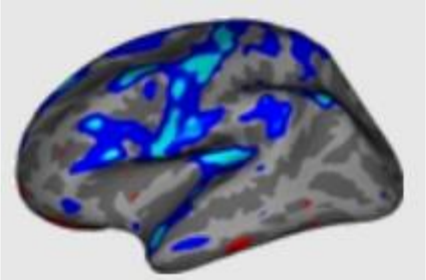

https://surfer.nmr.mgh.harvard.edu/

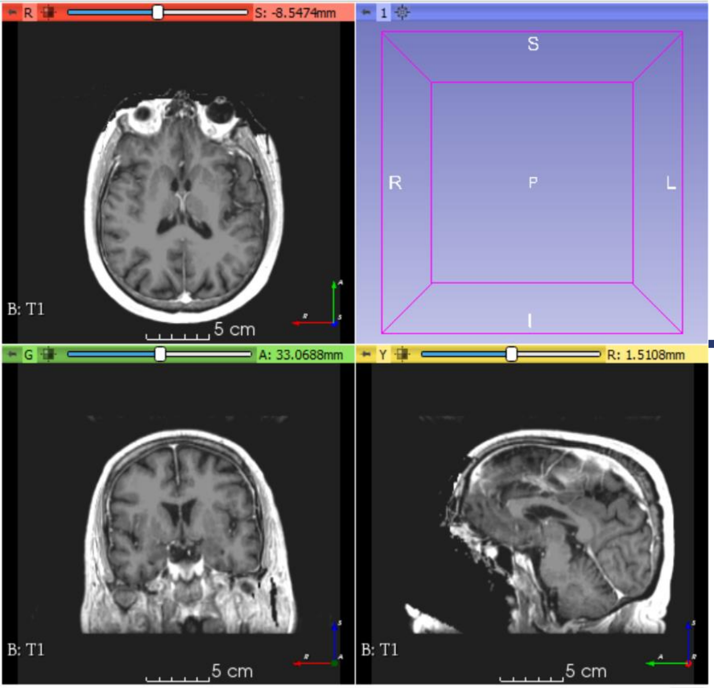

Automatic subcortical segmentation

Automatic procedure that classifies the voxels of a given brain MRI scan in ~40 labels corresponding to regions of the brain. It is based on:

- a probabilistic atlas of structure locations
- anatomically-robust registration

Further details in:
Fischl et al., Neuron, 33:341-355 (2002).

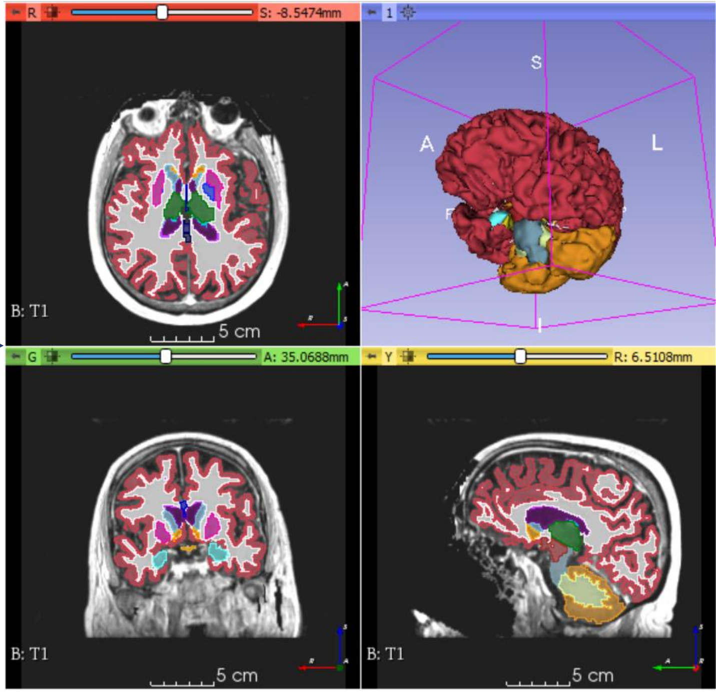

FreeSurfer for automatic region reconstruction

FreeSurfer

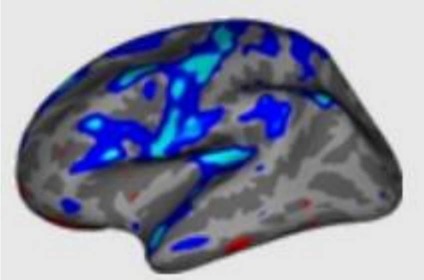

https://surfer.nmr.mgh.harvard.edu/

- Given an MRI, we can identify different brain regions automatically with the following command (running takes 12-24 hours)

  `recon-all -subjid out-directory -i T1.mgz -all`

- The output to this command contains a lot of information and statistics: we are using the tags contained in

  `out-directory/mri/aseg.mgz`

  (available in the shared folder)

- We can visualize and further process the result in 3DSlicer, enabling the SlicerFreeSurfer extension from

  3DSlicer menu View – Extension Manager

FreeSurfer for automatic region reconstruction – results

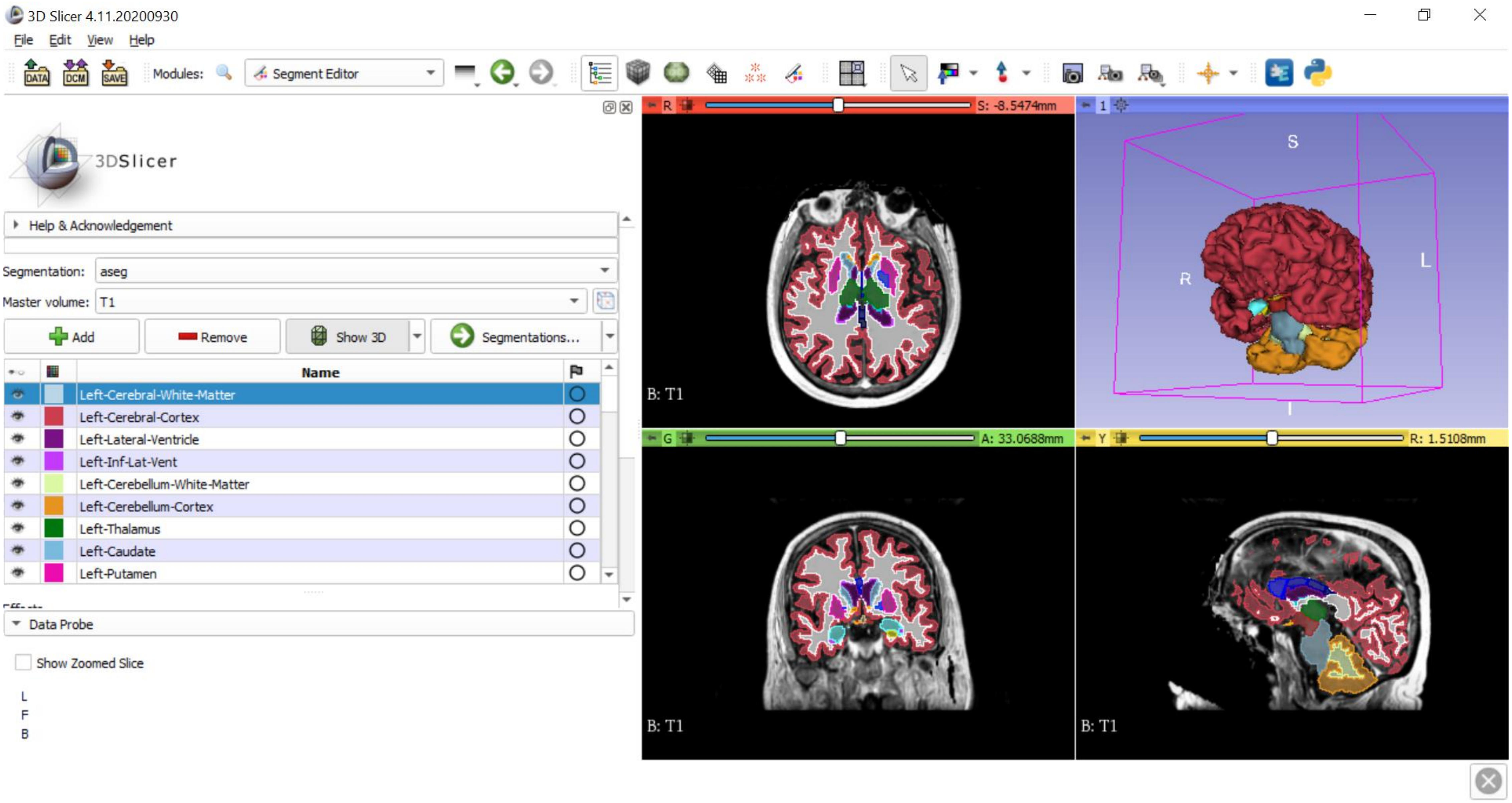

2.2 – Surface processing and mesh generation

From segmentations to a computational mesh

- In 3DSlicer, the content of aseg.mgz is called *Segmentation* and the single labeled regions are *Segments*
- We can combine and modify segments to create surfaces containing the complete grey matter, white matter, and brain ventricles, and then export them as STL surfaces (see shared folder)
- These surfaces can contain defects: a first, rough cleanup can be done in Paraview

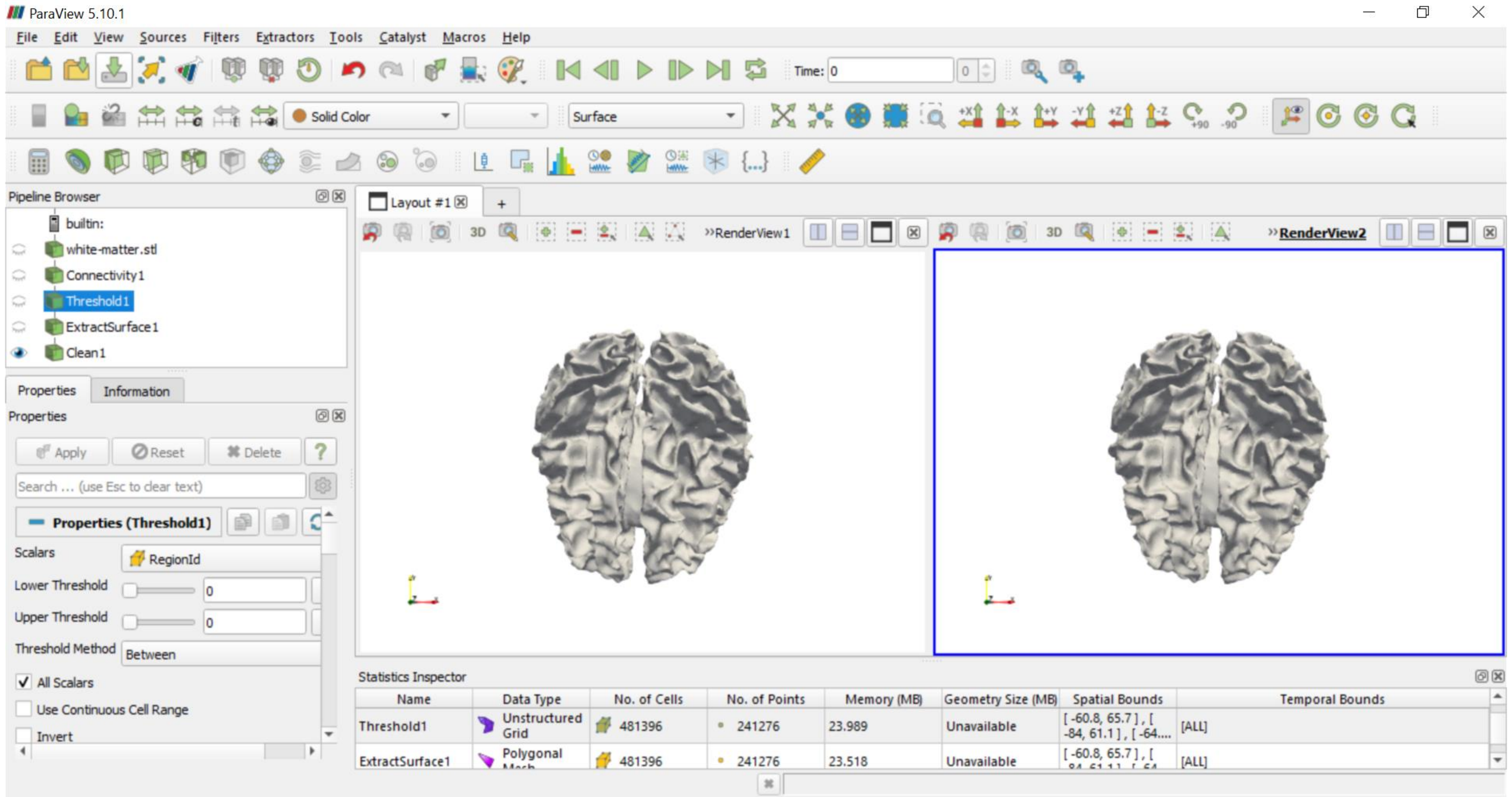

Note: the segmentation of the **ventricles** in 3DSlicer requires **significant manual work**. A full ventricle segmentation is provided in the shared folder.

The Surface Volume Meshing Toolkit (SVMTK)

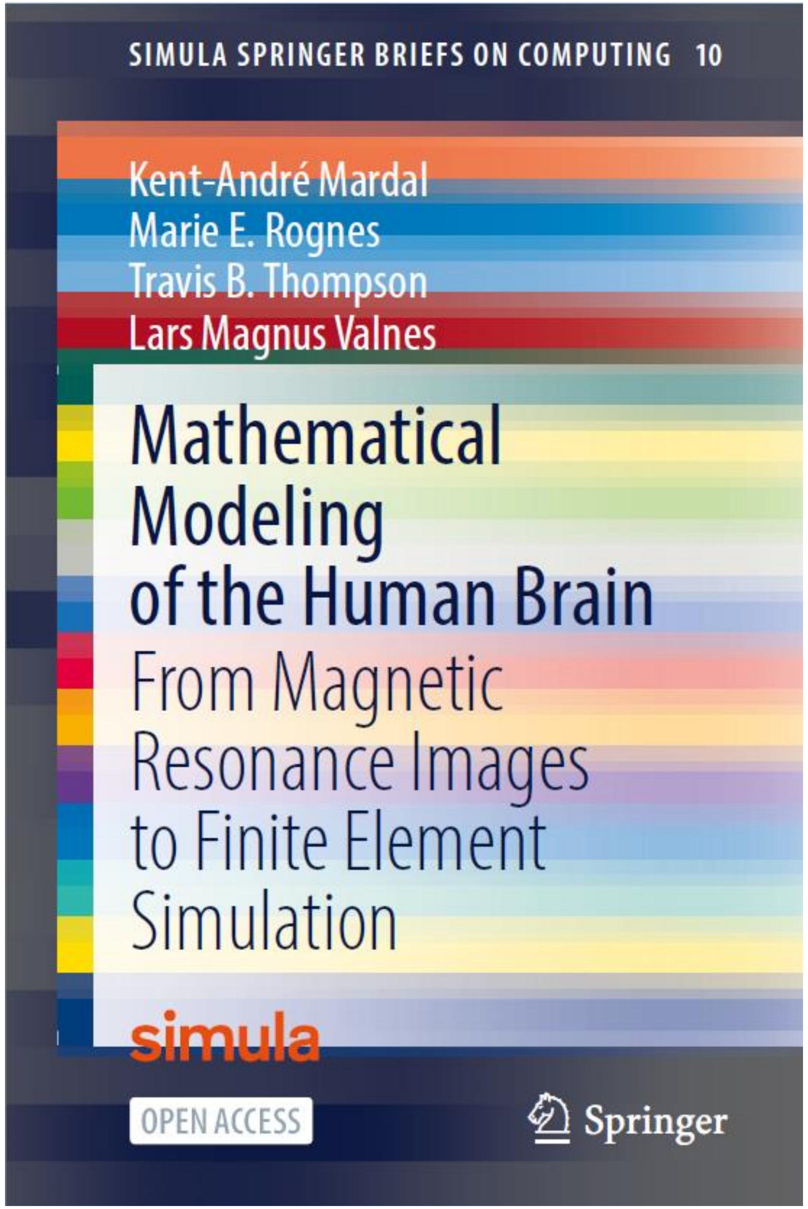

[Mardal, Rognes, Thompson, Valnes (2022)]

https://github.com/SVMTK/SVMTK

SVMTK is a Python library for **surface processing and mesh generation** based on the Computational Geometry Algorithms Library (CGAL). It is designed to create volume meshes of soft organic tissue surfaces, like the **human brain**, with the option to **repair unphysical errors** on the surfaces.

Files and formats

SVMTK

- .stl broadly employed format for triangulated **surface**
- .mesh (2D/)3D **mesh** in the format used by FEniCS https://fenicsproject.org/

ParaView

- .vtp VTK (**not** SVMTK) format for triangulated **surface**
- .vtu VTK (**not** SVMTK) format for tessellated **mesh**

Format conversion by meshio

Surface processing – common issues

Surface smoothing

original

Taubin smoothing

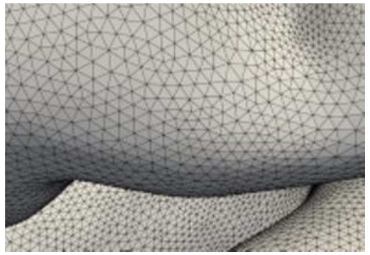

Laplace oversmoot’g

Prevent self-intersection

narrow gaps

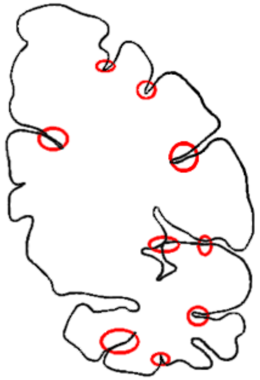

- **fill** holes (useful to remove **internal** artifacts)
- **separate** narrow gaps (useful for **sulci**)

[Mardal, Rognes, Thompson, Valnes (2022)]

Multi-domain geometry

Combining multiple surfaces

- Surface processing (smoothing/holes) should also account for intersections **across surfaces**
- Volumes are defined as inside (1) or outside (0) a given surface

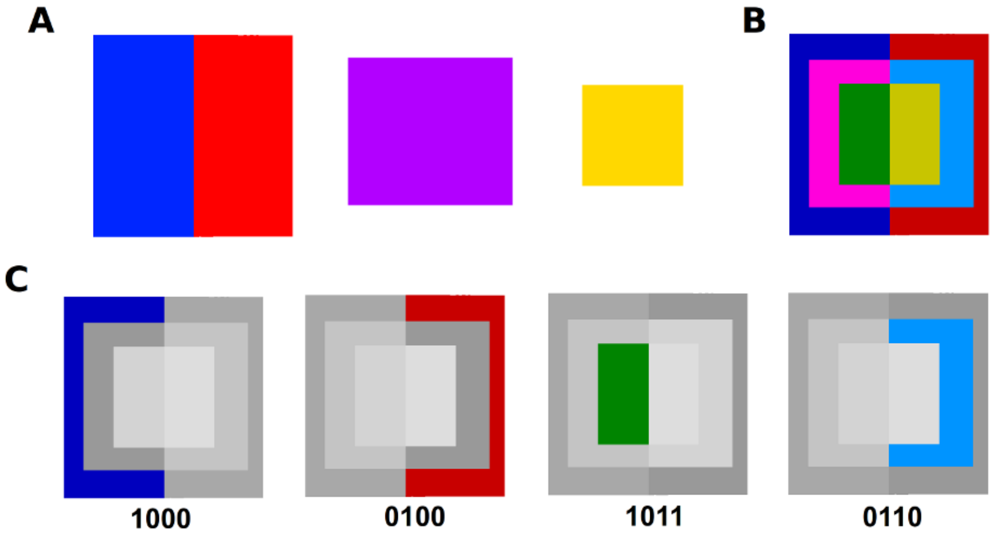

[Mardal, Rognes, Thompson, Valnes (2022)]

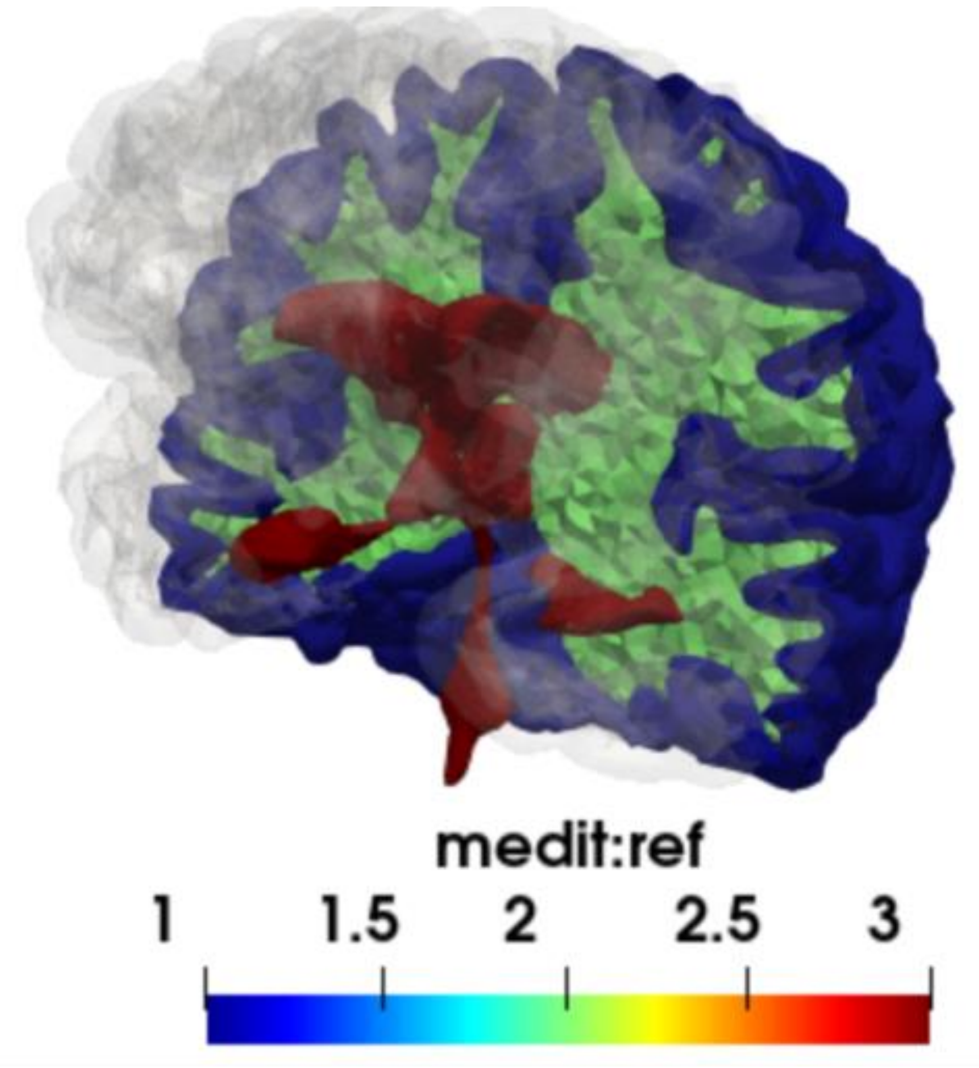

Computational results: brain perfusion and CSF flow

- displacement and Stokes source terms
  $\boldsymbol{f}_{el} = 0$, $\boldsymbol{f}_{f} = 0$
- **distributed CSF source**:
  (interstitial) CSF pressure source term
  $\boldsymbol{g}_{el} = c_P\, 2\pi \cdot 10^3 \sin(2\pi\, t)$ [s^{-1}]

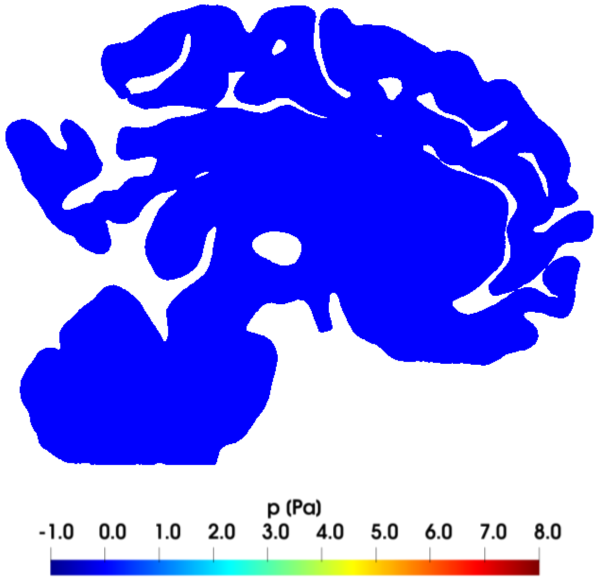

- displacement ~ 0.01 mm
- (-) pressure gradient **towards brain ventricles** until t ~ 0.7s
- **oubtound flow**
- ~ **continuous pressure** at interface

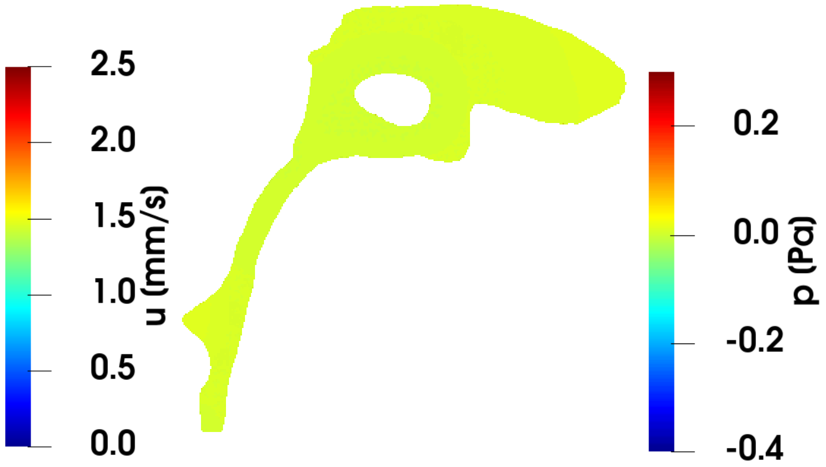

Computational results: brain perfusion and CSF flow

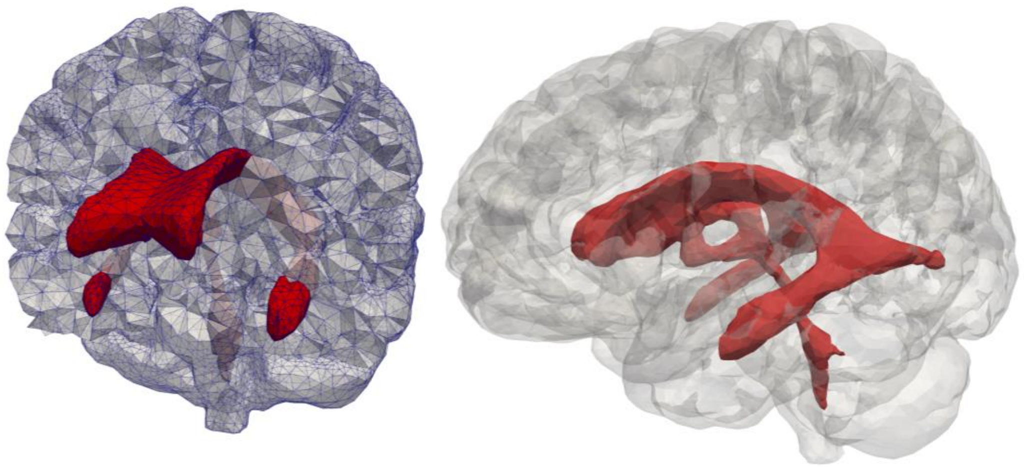

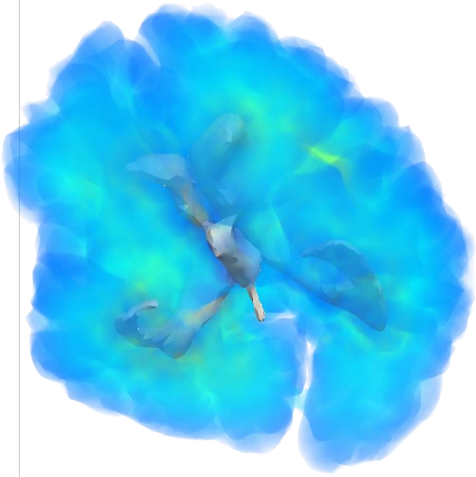

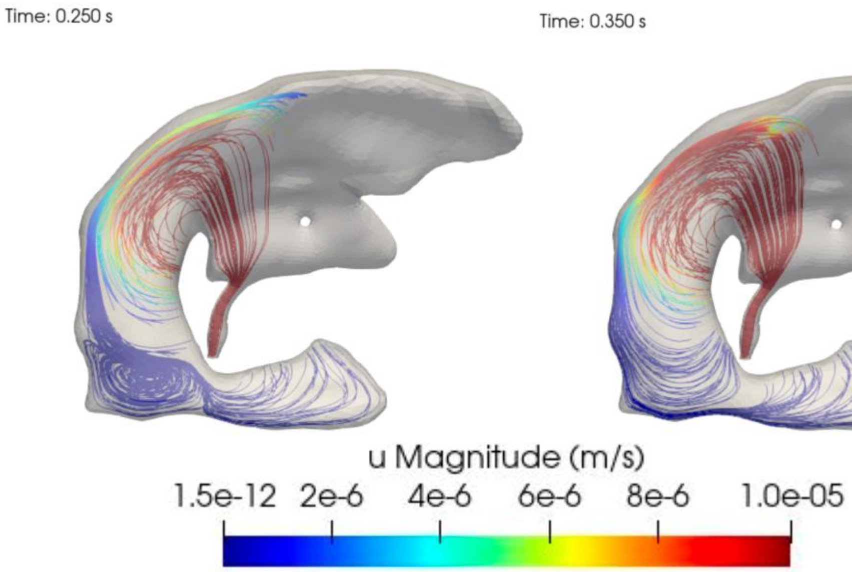

Credits: I. De Vittori

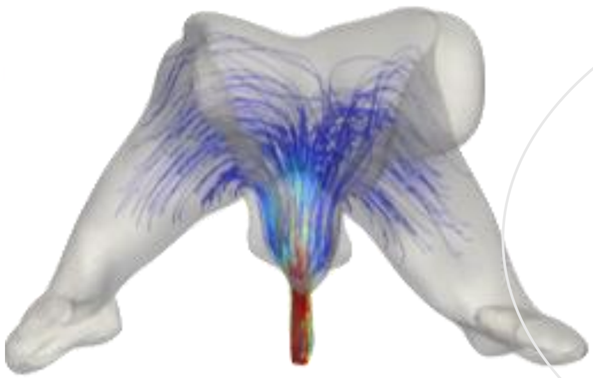

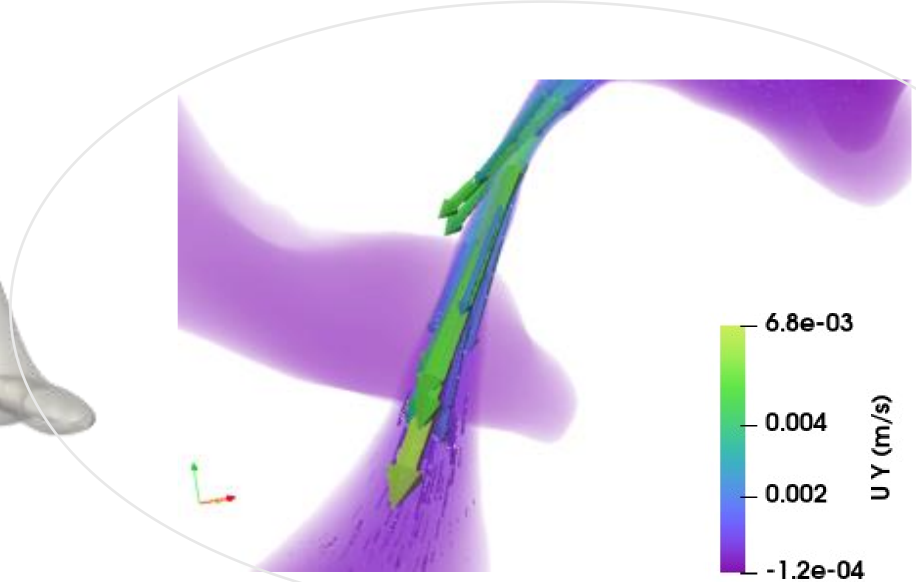

Zoom in the aqueduct of Sylvius. Credits: E. Irali

3 – Computational modelling of brain hemodynamics

Blood flow in the brain

- Blood flow supplied by (left/right) **carotid and basilar arteries**
- Medium-sized vessels: **Circle of Willis** (CoW)
  - Arterial **network** at the base of the brain
  - Circular structure: **redundancy** to preserve perfusion despite vessel **occlusion**
  - Incomplete CoW in >50% adults (also in the physiological case)

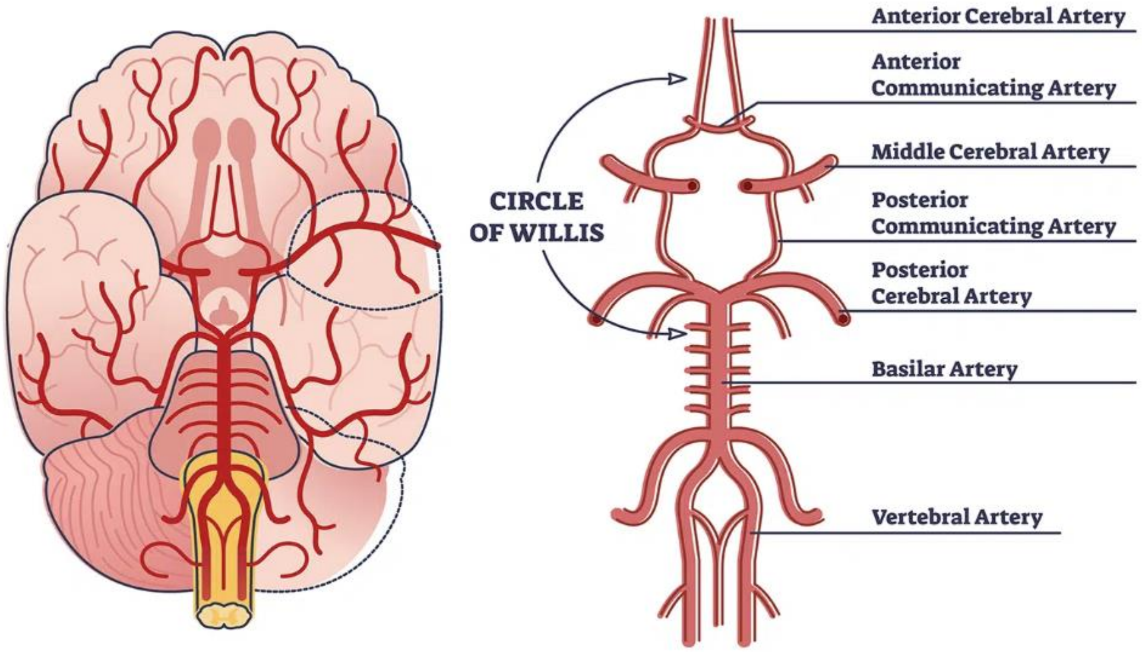

Benchmark geometry (⌀ 0.8-2.0 mm)

[Figueroa (2020) https://doi.org/10.7302/xx1r-zg70]

Blood flow in the brain – 1D

[R.Petrucci, MSc Math.Eng., PoliMI (2024)
L.Mueller, E.Toro, IJNMBE (2014)
G.Bertaglia, V.Caleffi, L.Pareschi, A.Valiani, JCP (2021)]

1D fluid-structure interaction model:

hyperbolic conservation laws for *Q* and *A* (Taylor-Galerkin disc.)

- assumptions: **linear elastic** walls, power-law profile
- discretization: 2nd-order **Taylor-Galerkin**
- BC: physiological *Q* (inflow), *P* (outflow) + compat. conditions
- **Branching**: nonlinear system (treated semi-implicitly, solved with Newton method

$$\begin{cases} \partial_t A + \partial_z Q = 0, \\ \partial_t Q + \alpha \partial_z \left(\frac{Q^2}{A} \right) + \frac{A}{\rho_f} \partial_z P + K_r \frac{Q}{A} = 0 \\ P - P_{\text{ref}} = \beta \frac{\sqrt{A} - \sqrt{A_0}}{A_0} \end{cases}$$

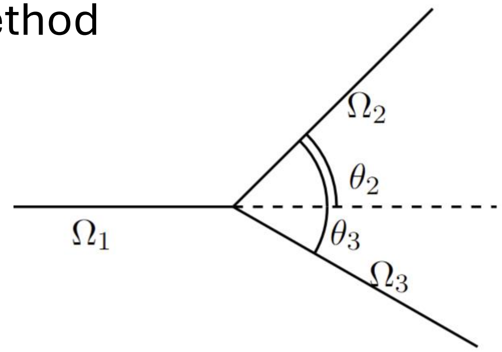

$$Q_1 = Q_2 + Q_3$$

$$P_{tot,1} = P_{tot,i} + \gamma_i \frac{Q_i^3}{Q_i A_i^2} \sqrt{2(1 - \cos\theta_i)}, \quad i = 2, 3$$

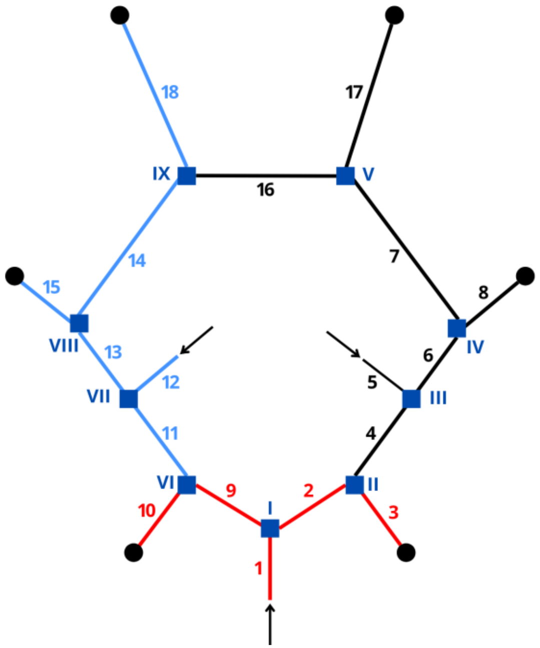

Blood flow in the brain – 1D – (preliminary) results

Modeling: dissipative effects of bifurcation angles

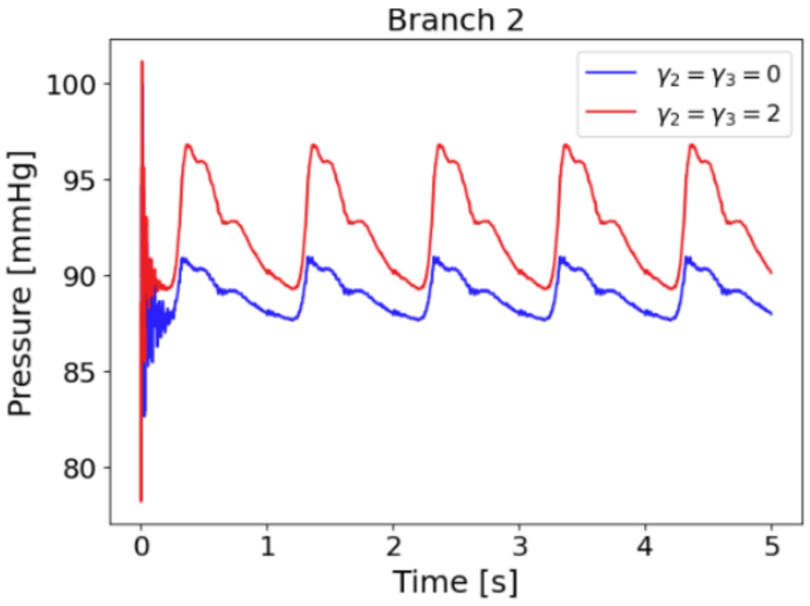

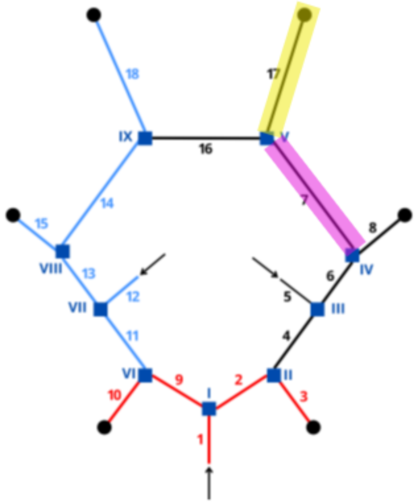

- including angles: reduced amplitude + better agreement with experimental measures [DeVault et al (2008)]

Application: effects of arterial obstruction

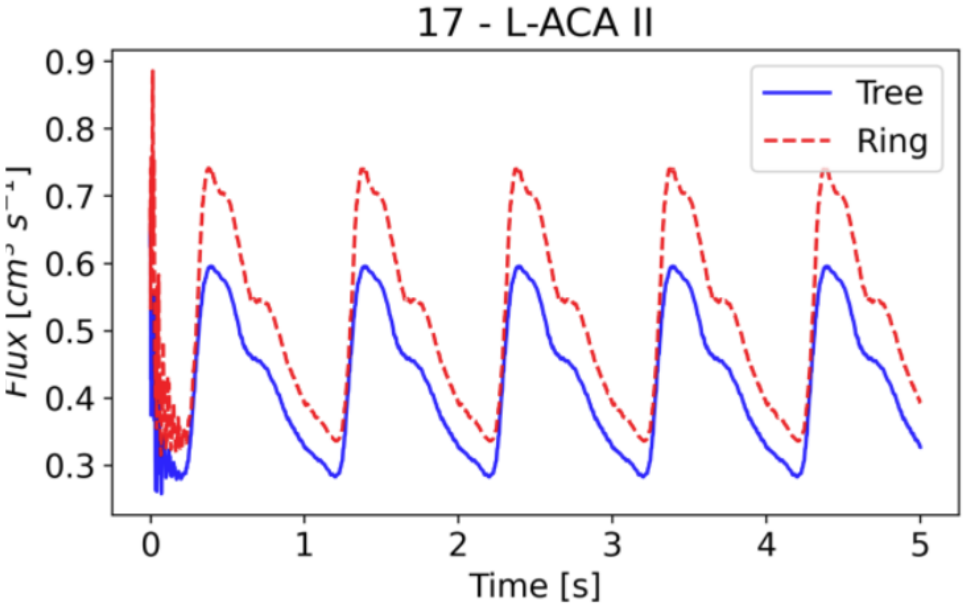

- incomplete CoW: >50% adults
- increased risk of neurological events
- reduced perfusion

Open issues

- surrounding cerebral tissue (viscoelastic effects)
- improve numerical method (order of accuracy, dispersion)
- calibration of branching model

[R.Petrucci, MSc Math.Eng., PoliMI (2024), L.Mueller, E.Toro, IJNMBE (2014), K.DeVault et al, Multiscale Mod Simul (2008)]

Blood flow in the brain – 3D

- 1D model is computationally inexpensive, but makes assumptions on
  - velocity profile
  - branching flowrate/pressure repartition
- **3D model** needed when **detailed flow** is of interest, e.g. for
  - cerebral aneurysm
  - amyloid plaques on vessel walls

[Figueroa (2020) https://doi.org/10.7302/xx1r-zg70]

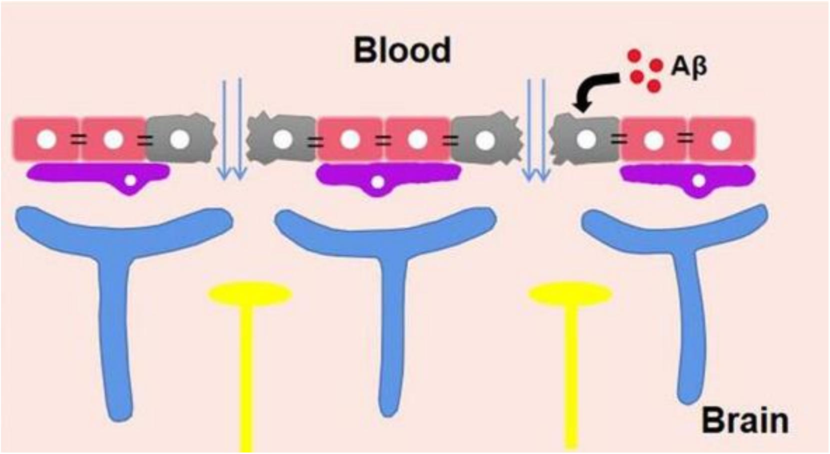

Vessel segmentation from clinical imaging data

1. Marching cubes algorithm (level-set front propagation): extracts the **surface polygonal mesh** from the isosurface at value zero of the *level set* image.

vmtk.org
github.com/checkrenzi/vmtk

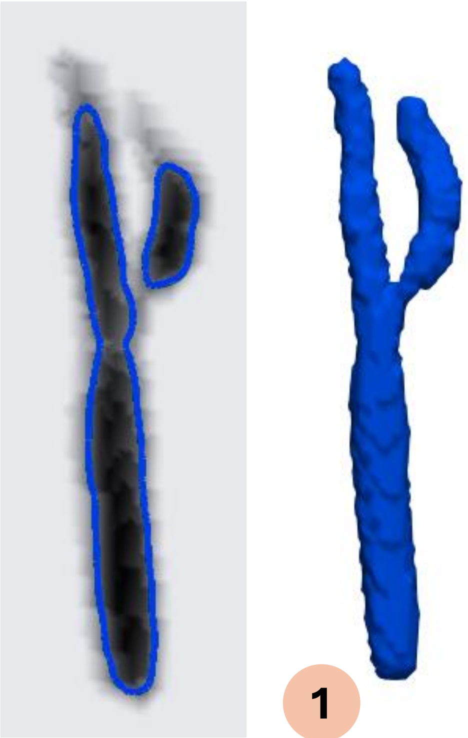

1

Vessel segmentation from clinical imaging data

1. Marching cubes algorithm (level-set front propagation): extracts the **surface polygonal mesh** from the isosurface at value zero of the *level set* image.
2. Smoothing: surface is artificially rough

vmtk

vmtk.org
github.com/checkrenzi/vmtk

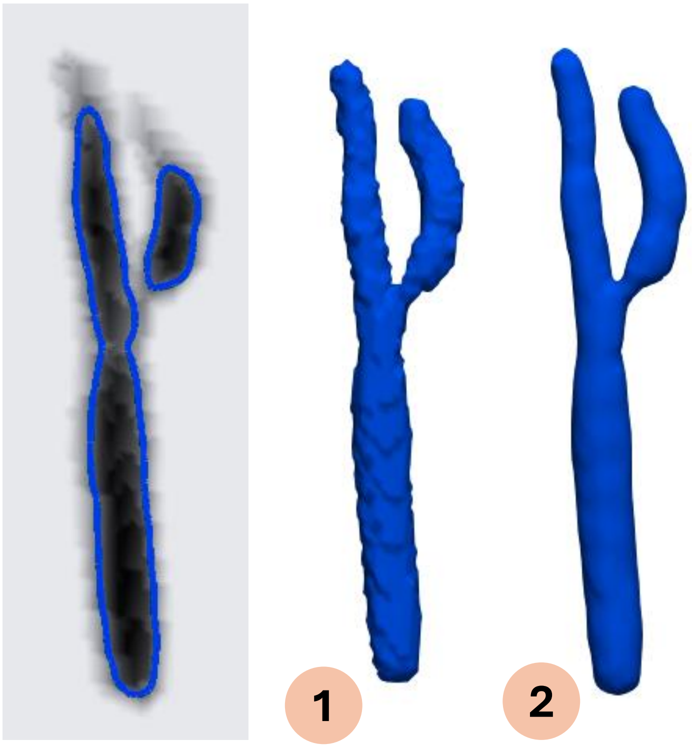

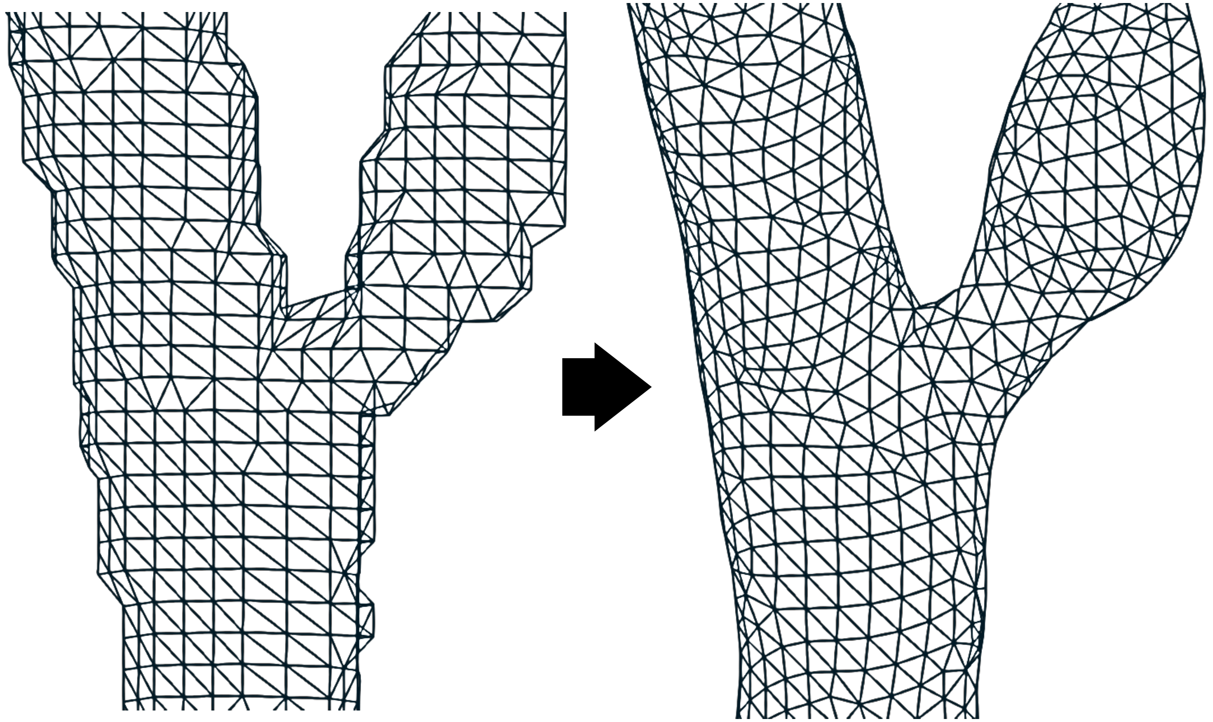

Vessel segmentation from clinical imaging data

1. Marching cubes algorithm (level-set front propagation): extracts the **surface polygonal mesh** from the isosurface at value zero of the *level set* image.
2. Smoothing: surface is artificially rough
3. Endpoint clipping

vmtk.org
github.com/checkrenzi/vmtk

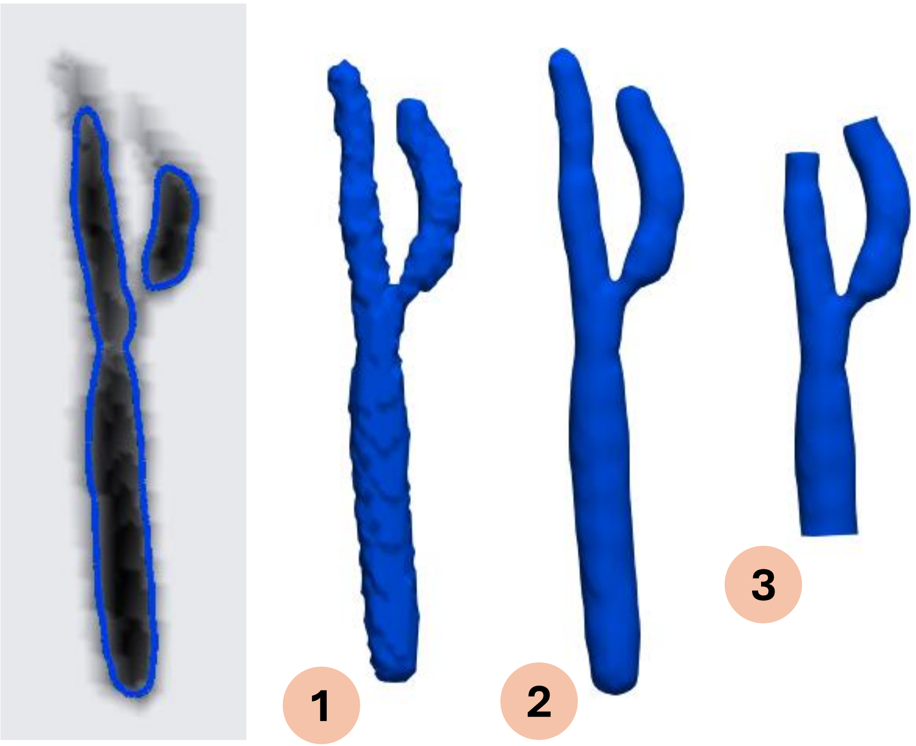

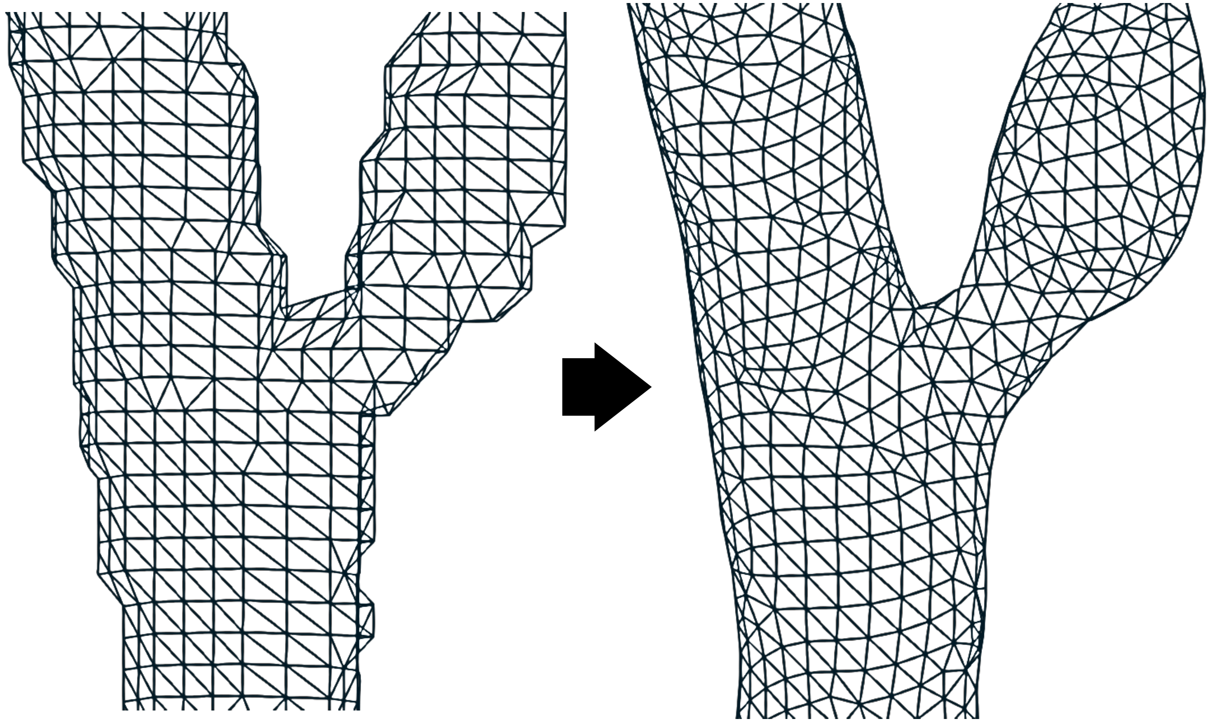

Vessel segmentation from clinical imaging data

1. Marching cubes algorithm (level-set front propagation): extracts the **surface polygonal mesh** from the isosurface at value zero of the *level set* image.
2. Smoothing: surface is artificially rough
3. Endpoint clipping
4. Flow extensions and/or centerlines
5. Surface remeshing

vmtk

vmtk.org
github.com/checkrenzi/vmtk

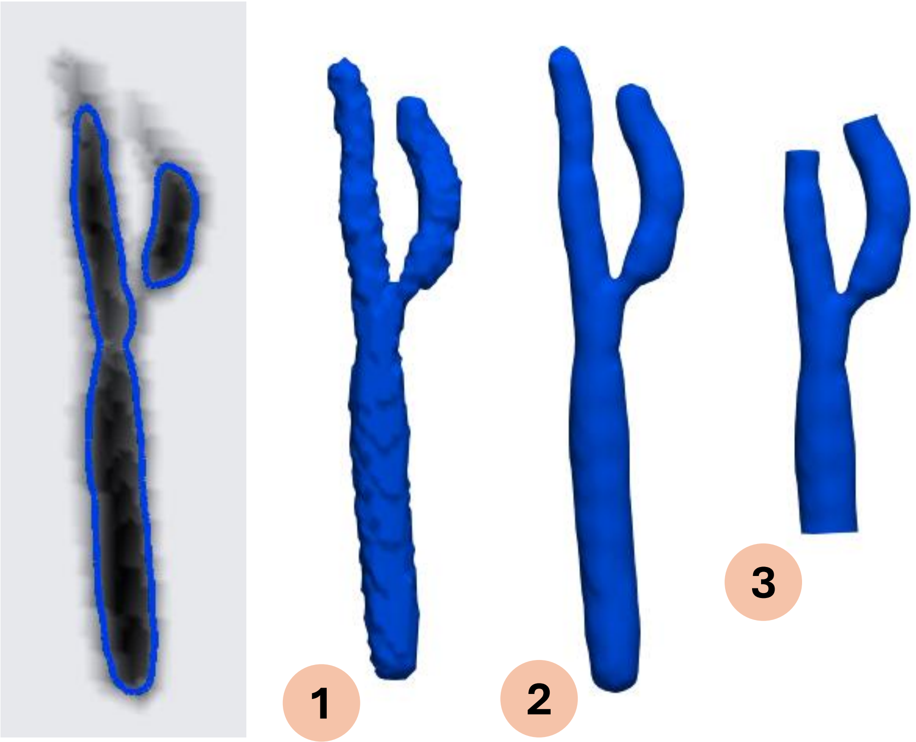

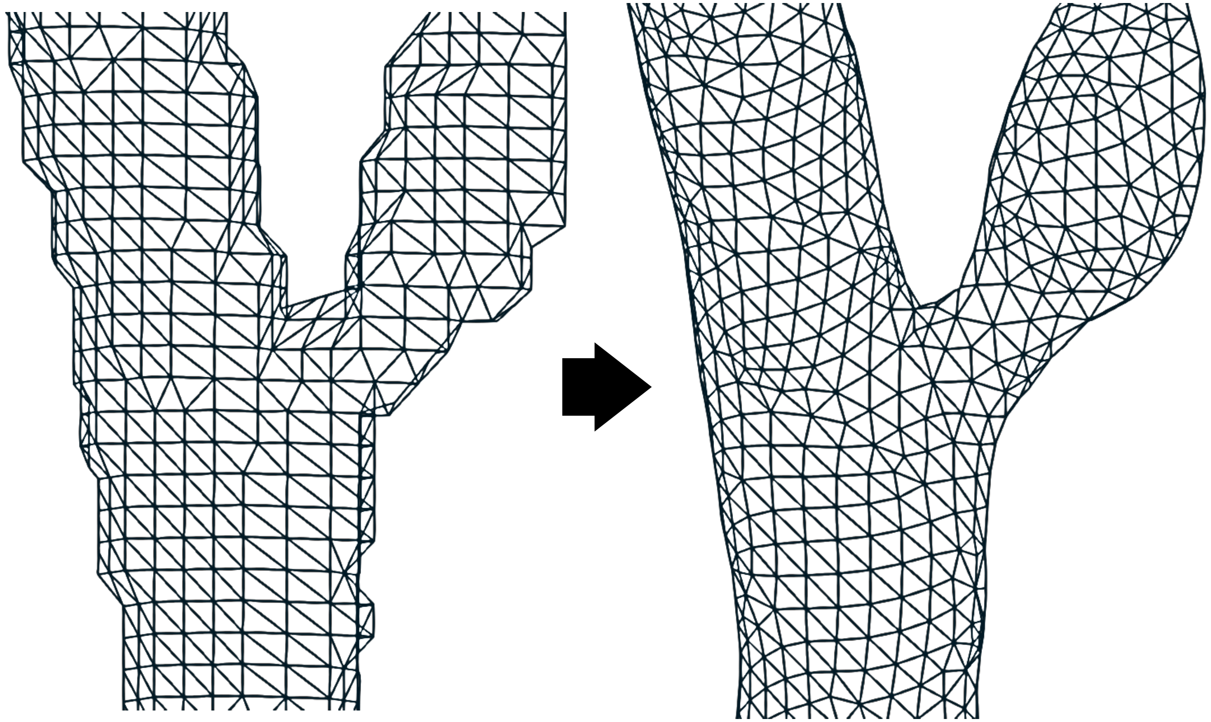

Mesh generation

- Automatic tetrahedralization of triangulated surface

  ⇨ many tools available on the market (e.g. tetgen)

vmtk

vmtk.org
github.com/checkrenzi/vmtk

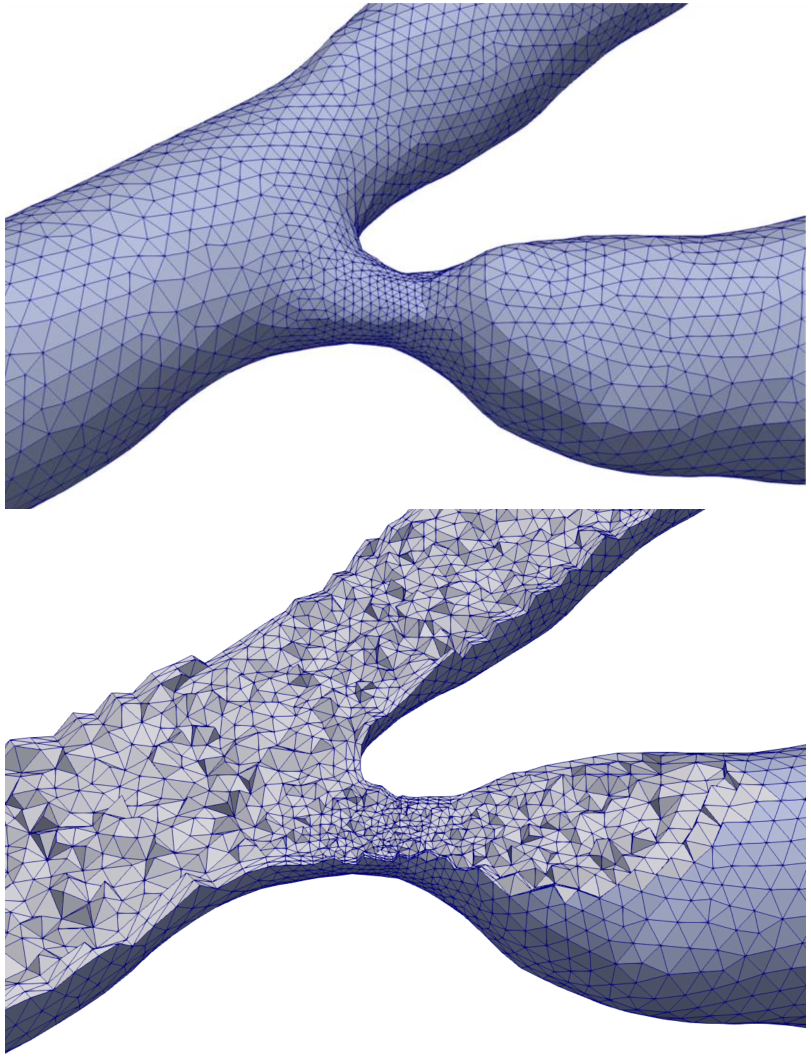

More complex meshing, involving a boundary layer, is required in some applications, e.g.

- CFD with accurate resolution of the flow boundary layer
- Fluid-structure interaction

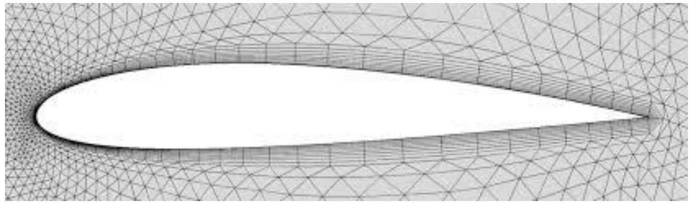

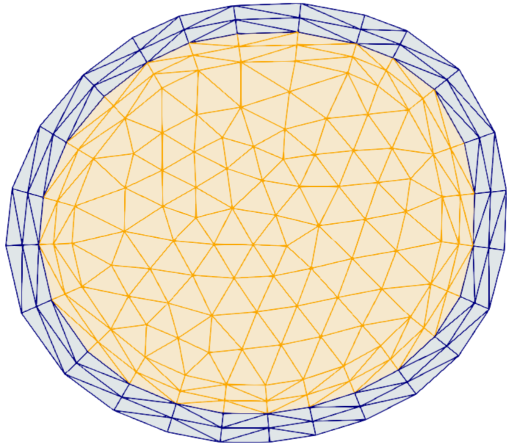

Fluid mesh

Solid mesh

Blood flow in the brain – 3D – results

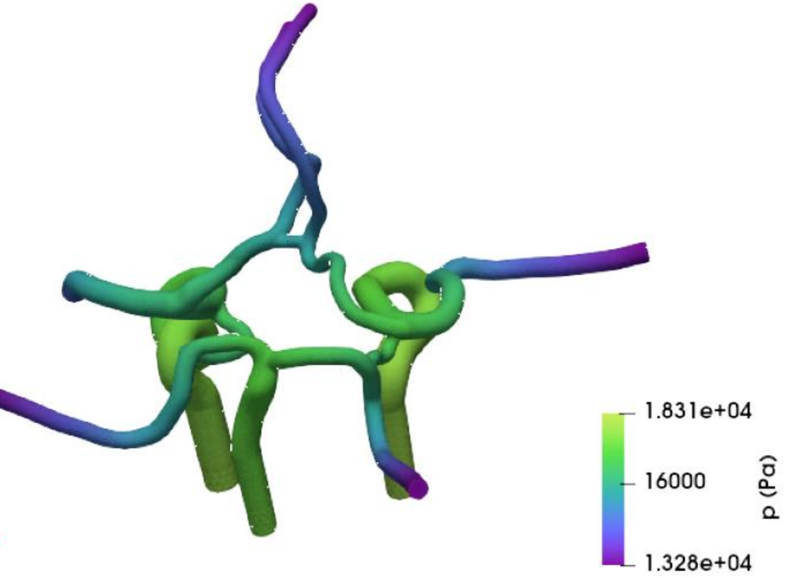

Horizontal component of the velocity in the cerebral arteries at t = 0.005 s.

[E.Irali, MSc Math.Eng., PoliMI (2024)]

Main references

- I. Fumagalli, M. Corti, N. Parolini, P.F. Antonietti (2024). *Polytopal discontinuous Galerkin approximation of multiphysics flow in the brain*. Journal Computational Physics 513, 113115 https://doi.org/10.1016/j.jcp.2024.113115
- I. Fumagalli (2024). *Discontinuous Galerkin method for a three-dimensional coupled fluid-poroelastic model with applications to brain fluid mechanics*. Submitted (preprint arXiv:2406.14041)
- P.F. Antonietti, S. Bonetti, M. Botti, M. Corti, I. Fumagalli, I. Mazzieri (2024). `lymph`*: discontinuous poLYtopal methods for Multi-PHysics*. ACM Transactions on Mathematical Software (accepted. Preprint arXiv:2401.13376)
- M. Corti, P.F. Antonietti, L. Dede', A. Quarteroni (2023). *Numerical modelling of the brain poromechanics by high-order discontinuous Galerkin methods*. Mathematical Models and Methods in Applied Sciences 33(8)
- E. Eliseussen, M.E. Rognes, T.B. Thompson (2023). *A posteriori error estimation and adaptivity for multiple-network poroelasticity*. ESAIM: Mathematical Modelling and Numerical Analysis, 57(4), 1921-1952.
- M. Causemann, V. Vinje, M.E. Rognes (2022). *Human intracranial pulsatility during the cardiac cycle: a computational modelling framework*. Fluids Barriers CNS 19
- K.A. Mardal, M.E. Rognes, T.B. Thompson, L.M. Valnes (2022). Mathematical modeling of the human brain: from magnetic resonance images to finite element simulation (Vol. 10). Springer Nature.
- W.M. Boon, M. Hornkjøl, M. Kuchta, K.A. Mardal, R. Ruiz-Baier (2022). *Parameter-robust methods for the Biot-Stokes interfacial coupling without Lagrange multipliers*. Journal of Computational Physics 467
- A. Cangiani, E.H. Georgoulis, P. Houston (2014). *hp-version discontinuous Galerkin methods on polygonal and polyhedral meshes*. Mathematical Models and Methods in Applied Sciences 24

ivan.fumagalli@polimi.it
brainum.mox.polimi.it

lymph.bitbucket.io
(open-source)

Acknowledgments

We thank L. Bennati, M. Corti, E. Irali, R. Petrucci, F. Renzi, I. De Vittori for their contributions to the graphics of this presentation and to the development of the presented tools. We acknowledge the use of open access imaging data by A. Taha et al. [OpenNeuro project ds004471]. This work has been partially funded by the Italian Research Center on High Performance Computing, Big Data and Quantum Computing (ICSC), under the NextGenerationEU project. The present research is part of the activities of "Dipartimento di Eccellenza 2023-2027", Dipartimento di Matematica, Politecnico di Milano. All the authors are members of INdAM-GNCS.